ABSTRACT

SWANEY, PAUL MICHAEL. Target and Core Optimization for an Electron Accelerator-Driven Transmutation Facility. (Under the direction of Dr. Man-Sung Yim.)

The current statutory limit for Yucca Mountain is quickly being met by waste produced at the reactors operating in the United States. A possible method of modifying reactor waste for more efficient storage in Yucca Mountain is transmutation. This study analyzes the use of an electron accelerator targeting its beam on a neutron producing target within a subcritical reactor fueled with transuranic waste from power reactor operations.

To maximize the transmutation effectiveness of the design, several loading patterns were analyzed for neutronics behavior and transmutation effectiveness. Designs utilizing multiple batches of fuel or multiple targets within the core were also analyzed.

The loading pattern analysis showed no clear beneficial loading pattern for the neutronics of the core; however, the results indicated that placing Curium within the innermost fuel assemblies improved the transmutation effectiveness of the core. The most effective loading pattern in terms of neutronics and transmutation effectiveness utilized Curium assemblies in the innermost locations, Americium assemblies in the second ring, and Neptunium and Plutonium assemblies in the outermost locations.

The use of multiple batches in the core layout demonstrated superior neutronics behavior but lacked in transmutation effectiveness. On the other hand, the use of multiple targets in the core did not exhibit the lower peaking factors expected and also performed poorly in the area of transmutation effectiveness. Most likely, these core

designs should be combined with more effective loading patterns to maximize their benefits.

When comparing electron accelerator based systems with proton accelerator based systems, the proton based systems have a significant advantage due to the higher neutron production efficiency within the target. However, economic and timeline considerations make the deployment of electron based systems attractive in specific scenarios.

Target and Core Optimization for an Electron Accelerator-Driven Transmutation Facility

by
Paul Michael Swaney

A thesis submitted to the Graduate Faculty of
North Carolina State University
in partial fulfillment of the
requirements for the Degree of
Master of Science

Nuclear Engineering

Raleigh, North Carolina

2007

APPROVED BY:

_____	_____
Dr. David McNelis	Dr. Ernie Stitzinger

_____
Dr. Man-Sung Yim
Chair of Advisory Committee

BIOGRAPHY

Paul Swaney was born in Statesville, North Carolina in the United States. He received his bachelor of science degrees in Nuclear Engineering and Applied Mathematics from North Carolina State University (NCSU) in May 2006.

Paul began work on his Master of Science degree in Nuclear Engineering in August of 2006 working under the direction of Dr. Man-Sung Yim at NCSU. Paul was also mentored in his work by Dr. David McNelis from the University of North Carolina-Chapel Hill. Paul's research included analyzing various core loading designs for an electron accelerator-based transmutation facility.

Paul loves playing soccer, annoying his cat Lily, and spending time with his friends. Paul plays in the co-ed and men's leagues of the triangle adult soccer league based out of Raleigh, NC. Lily is a domestic long hair cat that hates to be petted. A lot of his friends are nerdy nuclear engineers as well, such as Jason Elkins, Tyler Schweitzer, his future roommate Brandon Clark, and Hope Gwatney; however, some of them are normal and in other degree programs.

ACKNOWLEDGEMENTS

The first people I would like to thank are my family members who have been supportive of me throughout my entire educational career. This extension of gratitude includes a thank you to my baby sister, Laura who made me go to half-priced sushi nights so often when I had other work to do.

I would also like to thank Dr. Man-Sung Yim and Dr. David McNelis who have both been very supportive during my work. Without their guidance and patience, I would not have been able to complete such an undertaking. Their patience and instructions during the weekly research meetings were my motivating factors throughout the project. I also appreciate the support of my math advisor Dr. Ernie Stitzinger, who worked with me on various administrative difficulties that arose during the completion of my math minor.

I would also like to thank all my friends who kept distracting me from my work. In particular, Brandon Clark and Jason Elkins for all the green tea runs, Peggle tournaments, and beta outings. Thank you as well to Hope Gwatney, my faithful research meetings secretary and beach buddy.

This research was financially supported through The Russell Family Foundation (TRFF).

TABLE OF CONTENTS

LIST OF TABLES

LIST OF FIGURES

1 INTRODUCTION

1.1 SPENT NUCLEAR FUEL DISPOSAL

In the United States, approximately 20% of electrical demand is met through nuclear power generation. There are currently 104 reactors operating within the US to meet this demand. During operations, nuclear reactors produce spent nuclear fuel (SNF) which is toxic, highly radioactive, and has high heat generation rates. The characteristics of SNF require special disposal methods to ensure public safety. In 1957, the US government began to look for an acceptable method to dispose of SNF waste. In the Nuclear Waste Policy Act of 1982, the US government decided a mined geological repository was the preferred method for disposal of high-level nuclear waste, including SNF.[1]

In 1983, the DOE began considering nine sites for use as repositories for nuclear waste. The DOE reduced the number of sites under consideration to five in 1986. Later that year, the Secretary of the DOE recommended three sites to the President for further consideration. In 1987, Congress amended the Nuclear Waste Policy Act. Under the amendment, Congress instructed the DOE to cease site characterization studies for the Hanford, Washington and Deaf Smith County, Texas sites. Yucca Mountain, Nevada became the only site studied by the DOE for use as a nuclear waste repository.[1]

Investigations into the feasibility of placing a geological repository in the Southwest began in the 1970s. In 1976, the director of the United States Geological Survey suggested several sites around the Nevada Test Site as possible candidates for a repository. Site characterization of Yucca Mountain started in 1986 and is ongoing today.[1]

The Nuclear Waste Policy Act limits the capacity of Yucca Mountain to 70,000 MTHM. This limit includes contributions from commercial SNF, SNF from research reactors, and High Level Waste from defense activities. Current plans allocate 63,000 MTHM of the limit to storing SNF from commercial reactor operations.[1] With the current fleet of operating reactors within the US, the limit for commercial SNF will be reached in 2014.[2] However, it is safe to assume most reactors will be operating beyond 2014 and new reactors will be built in the future. Therefore, the current legal capacity of Yucca Mountain for commercial SNF is not sufficient. However, given the past legal and regulatory complications associated with the construction of the repository at Yucca Mountain, there will likely be only one repository built in the US. Therefore, utilizing transmutation technologies to reduce the amount of waste to be disposed of at Yucca Mountain is important.

1.2 SNF COMPOSITION

In order to determine a method for increasing the capacity of Yucca Mountain, the factors limiting Yucca Mountain's capacity must be analyzed. All commercial reactors operating in the US today are light water reactors (LWRs). An LWR uses fuel composed of enriched uranium to generate electricity. The enriched uranium is composed of ~5% ^{235}U and 95% ^{238}U by weight. During fuel utilization within the reactor, the fission process transmutes the uranium primarily into fission products (FPs) and isotopes with higher atomic numbers. Isotopes with higher atomic numbers than uranium are termed transuranics (TRUs). However, the largest component of SNF is uranium, composing 95.5% of the SNF. The uranium in SNF is ~0.8% ^{235}U by weight, slightly higher than natural uranium (~0.7%). Figure 1 graphically shows the various constituents of SNF.

Plutonium and the minor actinides (MA) represent the TRUs present in SNF. The stable or short-lived fission products, and other long-lived fission products represent the FPs present in SNF and account for all material besides uranium and TRUs.

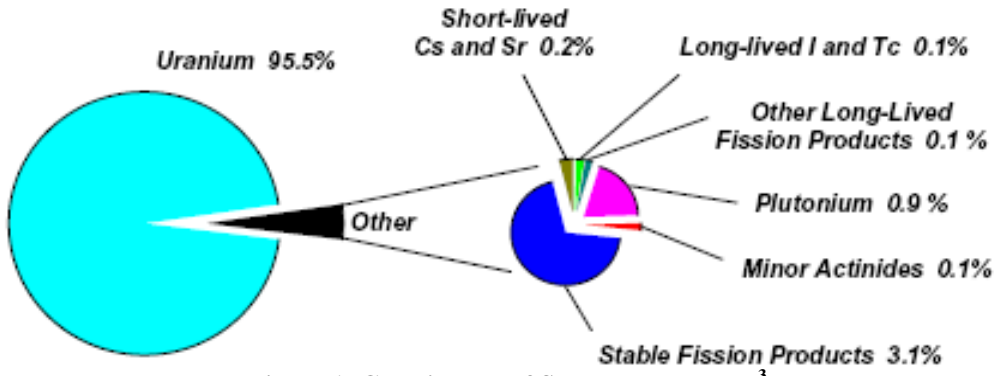

Figure 1: Constituents of Spent Nuclear Fuel[3]

The TRUs in SNF are produced by neutron capture and beta decay within the reactor. Neutron capture, which usually occurs as a (n,γ) reaction, results in new isotopes of the same element being produced. Beta decay increases the atomic number of the atom but maintains the same mass number. Therefore, for instance, in a reactor when ^{238}U undergoes a neutron capture, ^{239}U is produced. ^{239}U then goes through beta decay to produce ^{239}Np which then beta decays into ^{239}Pu, the most abundant isotope, other than ^{238}U, in SNF. All of the TRUs in SNF are produced in similar ways and they are all unstable. The unstable TRUs decay via alpha decay, beta decay, or spontaneous fission, although beta decay is the dominant mode.

Fission products are the resulting atoms from the fission processes occurring within a nuclear power reactor. Most FPs present in SNF are produced either directly from the fission process or as part of the decay chain of another FP. FPs are typically

neutron rich and therefore undergo beta decay to increase stability. There are several hundred different isotopes produced as FPs in a nuclear reactor.[4]

1.3 LIMITING FACTORS FOR REPOSITORY CAPACITY

The limiting factors for a geological repository are the radiotoxicity and heat generation of the SNF placed in the repository. Since all TRUs and most FPs are unstable, and therefore decay, they contribute to the radioactivity and heat generation of the SNF.

The radiotoxicity of the SNF is an indication of the potential adverse effects radiation from the SNF will have on living organisms.[4] The intake of radionuclides can occur for humans through two major pathways, inhalation and ingestion.

When analyzing the proposed Yucca Mountain repository, the most likely pathway for the release of the SNF to the environment is by ground water transport. Some of the radionuclides are water soluble and can be transported in the ground water away from the original disposal site. The radionuclides can then be ingested by either drinking the contaminated ground water or eating any food that relied on the contaminated ground water as its water supply.[4] Therefore, ingestion is the primary hazard associated with the disposal of SNF in the Yucca Mountain repository. Figure 2 shows the total ingestion toxicity of SNF will not have decreased to the level of natural uranium after a million years. The fission products ^{99}Tc and ^{129}I, both water soluble, are concerns for potential health risks due to their high migration rate in ground water. ^{237}Np, a TRU, is also of particular concern for its possible health effects. ^{237}Np can become more soluble in ground water depending on the pH level and oxidizing potential of its environment.[4]

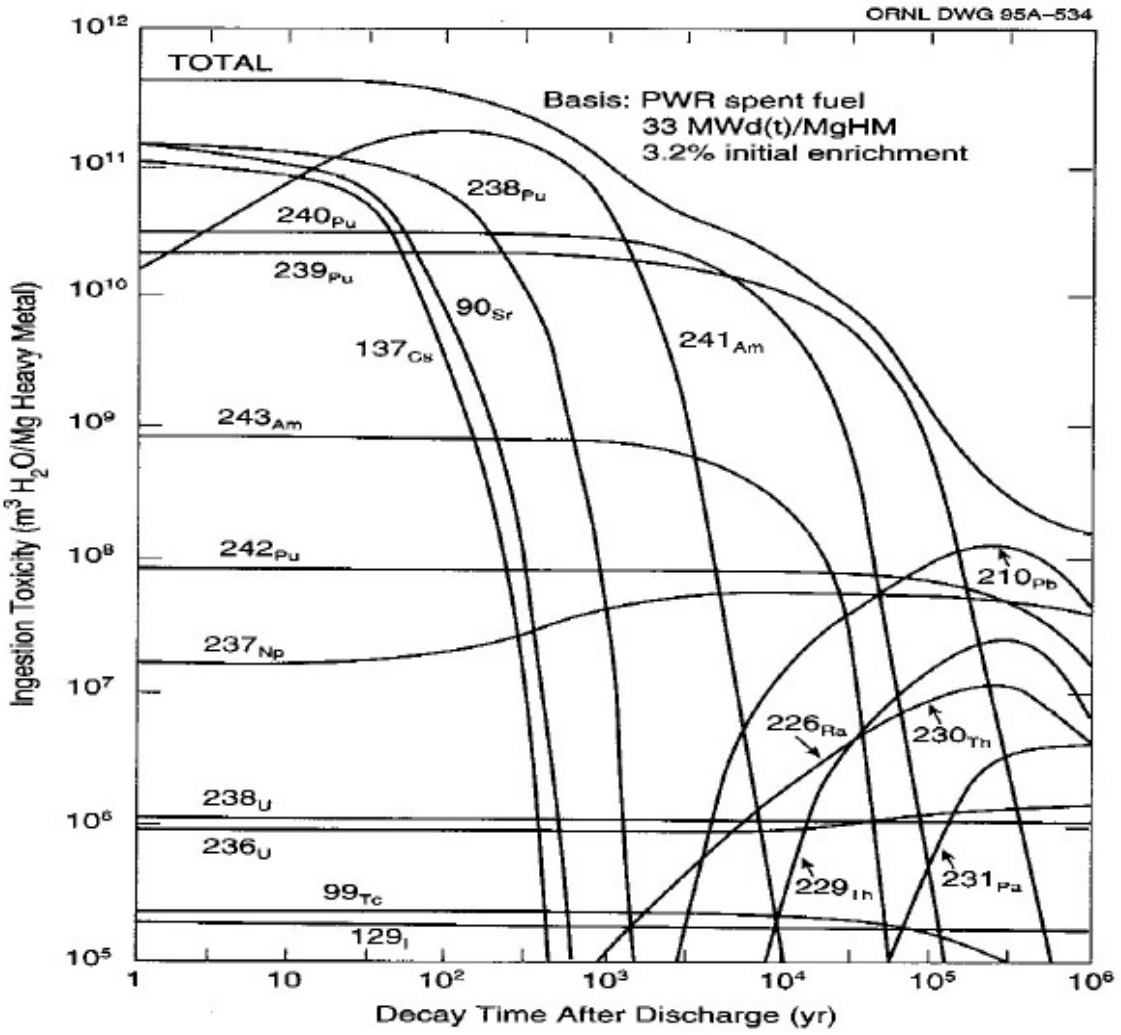

Figure 2: Ingestion Toxicity of SNF Constituents with Time[5]

The second factor limiting performance at Yucca Mountain repository is the decay heat generated by the SNF. When the various isotopes decay, heat is generated. The heat generation within the fuel raises the fuel temperature and the mountain's temperature around the fuel. However, due to fuel integrity and groundwater transport between drifts concerns, there are statutory limits on the maximum temperature allowed at various locations within the repository. Therefore, the heat generation of the SNF limits the amount of waste that can be placed within the repository while still meeting the temperature regulations. Figure 3 shows the decay heat generated by the SNF as a

function of time. On the figure, the decay heat attributed to various components such as actinides and ^{90}Sr+^{137}Cs are identified. [References on Figures]

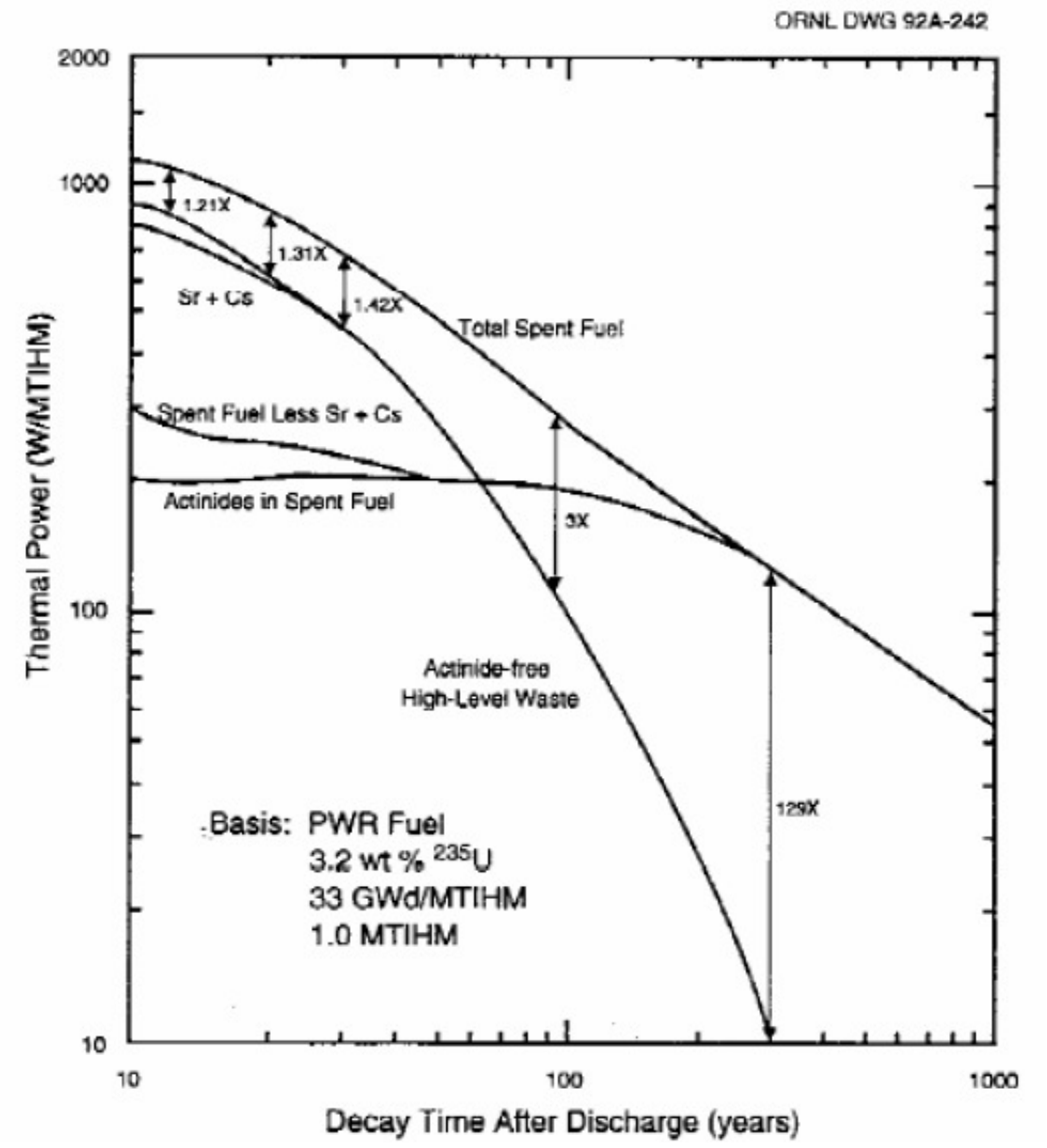

Figure 3: Decay Heat Generated by SNF and Constituents[6]

Figure 3 demonstrates that ^{90}Sr and ^{137}Cs dominate the decay heat generation by SNF in the short term (~100 yrs); however, in the long term the actinides present in the SNF are the biggest contributors to heat generation. ^{90}Sr and ^{137}Cs are two fission

products present in SNF. Therefore, when analyzing the radiotoxicity and heat generation of the SNF constituents, it is clear that ^{90}Sr, ^{137}Cs, ^{90}Tc, ^{129}I, uranium, and the TRUs are the components threatening repository performance due to the ingestion radiotoxicity and heat generation of these isotopes.

1.4 TRANSMUTATION

Transmutation is the conversion of one isotope into another of the same or a different element. The isotopes threatening repository performance mentioned above were created by transmutation of fuel within a nuclear reactor. However, further utilization of transmutation can help alleviate the impact certain isotopes will have on the repository performance. Transmutation can convert the most damaging isotopes into isotopes that are less radiotoxic, produce less heat, have shorter half lives or are stable. Transmutation can be induced by bombarding a material with various particles including alpha and beta particles, photons, or neutrons. Due to the high coulomb barrier associated with charged particle interactions and low photon cross-sections of the isotopes of interest, this study focuses on the use of neutrons for the required transmutations.

Neutron induced transmutation can be implemented in various methods using either a fast or a thermal flux. However, for ^{90}Sr and ^{137}Cs both the fast and thermal cross-sections are small enough to discourage transmutation. ^{90}Sr and ^{137}Cs are also two of the relatively shorter live isotopes mentioned affecting repository performance. Therefore, the scope of this study has been reduced to investigations regarding the transmutation of ^{90}Tc, ^{129}I, and the TRUs via neutron exposure. However, for most

transmutations concepts fuel reprocessing is assumed and therefore the uranium present in SNF is assumed to be recycled and reused in the fuel cycle.[4]

^{99}Tc and ^{129}I decay quickly to stable isotopes after neutron capture. ^{99}Tc and ^{129}I have high neutron capture cross-sections in the thermal region. Therefore, using a thermal flux for transmutation would be most effective for the fission products ^{99}Tc and ^{129}I. Neutron capture does not result in stable isotopes or a beneficial decay chain for the most abundant TRUs in SNF. Fission is the most effective means of transmutation for the TRUs. The fission cross-section for the TRUs is lower in the thermal region than in the fast region. In addition, the capture cross-section for TRUs is high in the thermal range. For any transmutation setup requiring effective neutron multiplication (criticality), the ratio of neutron capture cross-section to fission cross-section becomes more important than the value of the fission cross-section alone. The capture to fission ratio for most of the TRUs is higher for a fast neutron spectrum than a thermal spectrum.[7]

1.5 POSSIBLE METHODS OF TRANSMUTATION

Transmutation can occur by bombarding the target material with a number of incident particles. However, for heavier elements the coulomb barrier requires uncharged particles for practical transmutation rates. This study concentrates on the bombardment of fission products and TRUs from SNF waste with neutrons. There are many possible designs utilizing neutron bombardment for the transmutation of fission products and TRUs from SNF. The methods for neutron-induced transmutation can be broken down into categories based on the energy range of the neutron flux utilized. Therefore, the three main categories for transmutation methods utilize thermal, epithermal, and fast neutron fluxes.

The most common method of transmutation proposed for components of SNF is the placement of the material into an operating reactor. The reactor provides a neutron flux on its periphery that is utilized to transmute the waste. Depending on the reactor design, the SNF can be exposed to a thermal, epithermal, or neutron spectrum. An example of transmutation utilizing a thermal flux from an operating reactor is the MOX program currently operating in the US. MOX assemblies utilize excess plutonium reserves from weapons programs or, if reprocessing is reintroduced in the US, from recycled materials, for fuel. The goal of the weapons-related project is a joint effort by the US and Russia to reduce the available amount of weapons grade plutonium. The plutonium is transmuted into other isotopes during its utilization for energy production within modified power reactors. The MOX program is an example of thermal neutron-induced transmutation; however, for reducing the radiotoxicity of the SNF the MOX fuel cycle is not very efficient. The plutonium component of the MOX fuel is greatly reduced, but other TRUs are produced in the process.[8]

Nuclear reactors can also provide epithermal and fast neutron fluxes for SNF transmutation. The placement of SNF constituents into a fast reactor would expose the waste to transmutation via a fast neutron flux bombardment. As mentioned above, exposure in a fast neutron flux is not practical for the fission products of interest. However, it is possible to transmute the TRUs present in the fast flux of an operating reactor. Another possibility is the placement of the fission products of interest within a moderating medium on the periphery of the fast reactor core. Therefore, the TRUs can be transmuted within the fast flux in the interior of the core while the fission products are exposed to a thermal flux for efficient transmutation on the core periphery. Exposure of

SNF constituents to an epithermal neutron flux within a reactor system is also possible. The most likely method for accomplishing an epithermal flux for transmutation purposes is the use of a reactor with a fast neutron flux. This can be accomplished by placing moderating material in the area of the SNF constituents within the reactor. For example, the use of CaHx has provided high transmutation rates for ^{99}Tc in some reactor experiments.[9]

Utilization of reactors for neutron-induced transmutation of SNF benefits from the economics associated with energy production within a reactor system. Another benefit of using a reactor for transmutation is the neutron multiplication that occurs within the reactor system. The neutron multiplication within the reactor core increases the neutron flux to which the SNF is exposed. However, transmutation within reactor systems requires a critical reactor core to operate. And operation of a reactor requires the criticality and safety requirements to be met. In order to maintain criticality within a reactor system, fuel containing fertile isotopes is typically used; however, fertile fuel produces waste during the reactor operations. If the primary objective of a transmutation facility is the reduction of waste for disposal, the utilization of a reactor system for transmutation is not very efficient due to the production of additional waste when using fertile fuels.

A possible design for transmutation that does not require the use of fertile fuels is an accelerator. The energy spectrum of the neutrons produced in an accelerator system can be determined prior to construction and therefore tailored for the most efficient transmutation of the SNF isotopes of interest. However, an accelerator system does not possess the benefits associated with a reactor system. Neutron multiplication in an

accelerator system is substantially lower than what is observed in a reactor system. Therefore, the neutron flux the waste experiences is limited to the capacity of the accelerator setup. The second major drawback to using an accelerator for transmutation is the energy required to operate the system. With a reactor system, energy is required to operate the plant; however, energy is also produced and can be utilized for electricity production. The sale of electricity from a reactor system can easily offset and surpass the cost of operating the plant. A pure accelerator system cannot reclaim the amount of energy used during particle acceleration from the target interactions.

A third possible method for producing neutrons to use for SNF transmutation involves coupling the reactor and accelerator systems together in order to gain the benefits of both systems. This setup, known as an Accelerator Driven System (ADS), uses an accelerator beam of either electrons or protons to strike a target within a subcritical reactor core. When the accelerator beam strikes the target, neutrons are produced which bring the reactor up to criticality. An ADS has the benefits of neutron multiplication and power production provided from having the sub-critical core while eliminating the need for fertile fuel due to the extra source of neutrons from the accelerator and target. The extra source of neutrons provided by the accelerator and target also allow for greater flexibility in the fuel design of the reactor core. Another benefit of the ADS is the safety feature provided by the accelerator and reactor coupling. Since the reactor core is designed to be subcritical at all times except when the extra source of neutrons is present, the reactor can easily be shutdown by turning off the accelerator beam. Shutting down the accelerator is a dependable method for returning the reactor to a subcritical position quickly thereby increasing the safety of the ADS.

1.6 ACCELERATOR DRIVEN TRANSMUTATION SYSTEM

The ADS concept attempts to bring together the advantages of a reactor system with those of an accelerator system. The ADS has the potential of neutron multiplication within the core which would increase the neutron flux to which the SNF waste is exposed. Like the power reactor system, the ADS also has the ability to generate sufficient heat for power production. The electricity production provided by the ADS system can be used to operate the accelerator system and any excess can be sold to support the overall operational and capital costs of the system. However, unlike a typical reactor system, the ADS does not require fertile fuel for sufficiently long cycle lengths. The accelerator part of the system provides an extra source of neutrons that can maintain criticality as the k_{eff} of the fuel decreases during transmutation. Figure 4 shows a simplified view of how an ADS is structured.

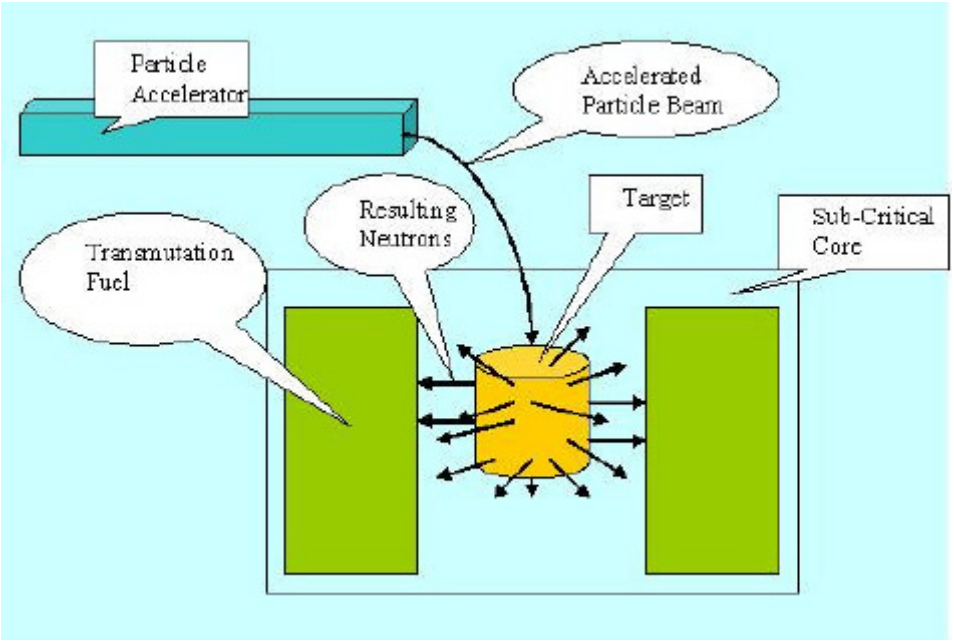

Figure 4: Simplified Schematic of an ADS[10]

There are two possible types of ADSs that can be utilized for SNF transmutation. The accelerator part of the system can be either an electron or a proton accelerator. An electron ADS uses Bremsstrahlung interactions within the target to produce the desired neutrons. The high-energy electrons interacting with the target material via Bremsstrahlung create a cascade of photons within the target. The photons then induce photon-neutron interactions (γ,n), producing neutrons, which are supplied to the surrounding subcritical reactor. On the other hand, the proton ADS uses the spallation process to generate the desired neutrons. The high-energy protons interact directly with the nuclei of the target material. Neutrons are ejected from the impacted nuclei and eventually are utilized with the subcritical reactor.

Either choice of beam particle has benefits over the other. Currently, a proton ADS is more efficient at producing neutrons in a target per incident proton from the accelerator. On the other hand, there is more of an experience base for electron accelerators. Electron accelerators are more widely used in the U.S. and, therefore, the experience base and development progress for electron accelerators is higher than for proton accelerators. These factors result in the electron accelerator having a higher operational stability than proton accelerators. Operational stability is very important for an ADS because the accelerator is coupled to a reactor system. When operating a reactor, unplanned shutdowns are to be avoided whenever possible. Therefore, having a more stable accelerator system is beneficial. Electron accelerators currently are also smaller and have lower capital costs than comparable proton accelerators.[11] Most conceptual ADSs currently utilize a proton accelerator due to their higher neutron production efficiency. However, this study investigates the possibilities for using an electron ADS.

An electron ADS may be deployable sooner due to the higher operational experience with electron accelerators. An electron ADS can also utilize smaller targets than a proton ADS and this effect on core design may favor an electron ADS.

1.7 PROPOSED SCOPE OF WORK

The goal of this project is to investigate factors in core design relevant to an electron ADS. As discussed further in Section 2, this study built upon the findings of two previous works by Yodersmith[10] and Liu[12]. Liu's work included a very detailed analysis of the electron interactions within the target and optimizing the neutron conversison efficiency. For Liu's analysis, a reference core design was utilized. Yodersmith expanded upon Liu's analysis be investigating more target material candidates and doing some preliminary loading pattern analyses for the subcritical core. These two studies provide sufficienct information on candidate target materials that more calculations were not required when determining the target material to utilize in this study. Therefore, the primary part of this study is devoted to analyzing the effect of core fuel loading patterns on the ADS in terms of overall criticality, criticality as a function of burnup, peaking factors within the reactor, and transmutation effectiveness. In all calculations performed for this project, a measure of the SNF transmutation rate or effectiveness were also performed. This study then quantified the effect of the various parameters on the transmutation effectiveness of the system. Unlike Yodersmith's study, this study developed loading patterns where Np was never separated from Pu due to proliferation concerns. This study utilized isotopic loadings that allowed the system to burn the various isotopes in ratios to each other similar to the ratio of their rate of production within spent fuel.

One of the possible benefits of using an electron ADS over a proton ADS is the smaller target size of the electron ADS. Therefore, using multiple targets is more feasible with an electron ADS. The possible benefits of using multiple targets within the core are better peaking factors and more flexibility in core design. This study also included an analysis of the effect of using multiple targets in the reactor core. In addition, an analysis to study the possible benefits of a multiple batch core for the electron ADS design was also performed which was not investigated in the previous studies. This type of study was not performed in Liu or Yodersmith's work. In this study, it was assumed that only a third of the core was reloaded during each outage, similar to currently operating power LWRs. The neutronics behavior and transmutation effectiveness of this approach was also studied. Overall comparison between electron ADS and proton ADS was performed and obervations were summarized at the end.

2 REVIEW OF PREVIOUS WORK

2.1 TARGET DESIGN

In the ADS design, the electron beam strikes a target within the subcritical core to produce neutrons, which drive the fission process. The design of the target involves many factors including compatibility with the core design, neutron production efficiency, and the system's transmutation efficiency. There are many aspects of the target affecting these factors, such as the target material, size, and shape.

The first aspect of an electron ADS target that must be determined is the target material. The target can be either liquid or solid. A target for an ADS is exposed to very high rates of energy deposition from the interacting accelerated particle beam. Therefore, the ability to cool the target is an important consideration when choosing a target material. A solid target in an electron ADS must be cooled using either reactor coolant or a separate cooling system. However, when using a liquid target, the target material can be constantly flowing into and out of the reactor vessel allowing for direct cooling of the fluid via heat exchangers outside of the reactor vessel. If a liquid target is utilized in the ADS design, it is possible to use the same flowing liquid as both the target material and core coolant. However, when using the same fluid as the target and core coolant, the presence of by-products from the neutron production within the core must be analyzed and accounted for. If a solid target is utilized for the ADS, then the target material may be the same as the reactor fuel. However, in order to maximize the neutron production efficiency of the target, the use of fuel material for the target is usually not practical.[10]

The target in an electron ADS is exposed to a flux of high energy electron particles from the accelerator and the high energy photons and neutrons produced during

the neutron production process involving Bremsstrahlung interactions. The exposure to these high energy particles results in a high rate of radiation damage within the target.[12] Since a liquid target would be continually flowing within the ADS design, the level of radiation damage can be managed more effectively. With a solid target, the target can only be replaced when the reactor is shutdown. However, a liquid target can be continuously processed during reactor operations to maintain the target's integrity.

In a proton ADS, neutrons are produced by the spallation process. In an electron ADS, the neutrons are produced from photons created by Bremsstrahlung interactions. The difference in the method of neutron production affects the amount of radiation damage a target for the respective systems is exposed to. Using MCNP modeling and the threshold energy for atom displacement, the radiation damage in an electron ADS target after 10Ah of exposure is R_{pep}=0.15±0.02 dpa and R_{pnp}=0.36±0.03 dpa.[12] Where R_{pep} is the peak radiation damage from electrons and R_{pnp} is the peak radiation damage from neutrons. This can be compared to radiation damage levels for a proton ADS target after 10Ah of exposure being R_{ppp}=9.41±0.34 dpa and R_{pnp}=8.03±0.29 dpa.[12] Where R_{ppp} is the peak radiation damage from protons and R_{pnp} is the peak radiation damage from neutrons. Therefore, the use of a liquid target to utilize its ability for constant online refurbishment is more beneficial in a proton ADS. The use of a liquid target in an electron ADS still has some benefits over a solid target, but not enough to rule out solid targets without looking at neutron production efficiency.

The target material used in an electron ADS is highly dependent on the material's ability to produce neutrons efficiently from the incident high-energy electrons. Yodersmith and Liu provide data regarding the target material design utilized in this

study to determine the design of the ADS target.[10,12] The candidate materials analyzed in the studies by Yodersmith and Liu their relationship to the core, and their reference article(s) are listed in Table 1.

Table 1: Candidate ADS Target Materials

Materials	Reference Analyzed In	Relationship to Core Design
Lead	[10,12]	Possible Coolant
Bismuth	[12]	N/A
Lead Bismuth Eutectic	[10]	Possible Coolant
Tungsten	[10,12]	N/A
Tantalum	[10,12]	N/A
Sodium	[10]	Possible Coolant
25w/o TRU in Zirconium	[10]	Possible Fuel
Thorium	[12]	N/A
Uranium	[10,12]	N/A

Table 1 showed that more candidate target materials were analyzed by Yodersmith that could serve a dual purpose as both the target and also either the coolant or fuel in the core. In the Yodersmith's study, the candidate target materials were subjected to an electron flux using MCNPX to determine the resulting neutron flux from the target's surface. The results of the target material study performed by Yodersmith are shown in Figure 5.

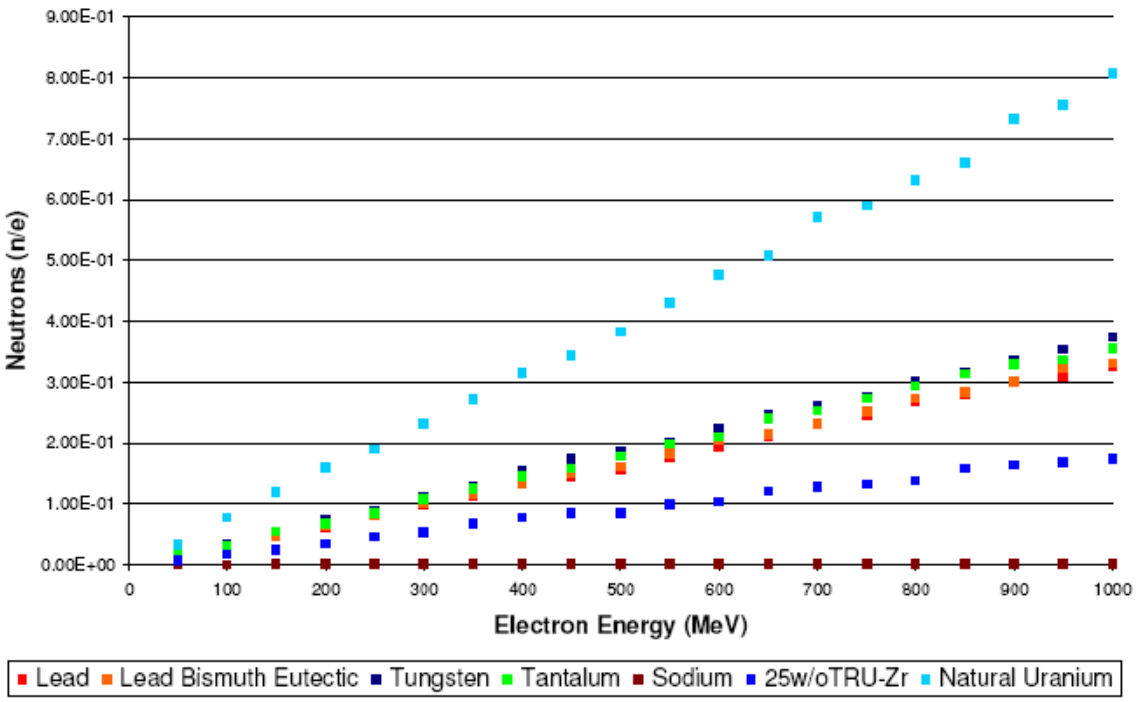

Figure 5: Target Material Neutron Production Efficiency Results [10]

The results in Figure 5 provide two important results. The first conclusion drawn from the figure is uranium has a much higher neutron conversion efficiency than any of the other target material candidates analyzed in the study. The second conclusion exhibited in the figure is there was a fairly linear correlation between the incoming electron beam's energy and the neutron conversion rate within the range of 50-1000MeV. In the analysis performed by Yodersmith, the electron ADS design used a Tungsten target. Tungsten was chosen as the ADS target material because it had the second highest neutron production efficiency after uranium. Uranium was not used in the study because of concerns that the byproducts of the neutron production reactions would inhibit the transmutation effectiveness of the electron ADS. During the neutron production within uranium, some capture reactions would occur producing the same TRUs the ADS was designed to eliminate. Therefore, uranium was not used as the target to ensure there was

no production of TRUs within the system. However, in the present study, the TRU production within a uranium target was considered along with the significant increase in neutron production efficiency possible with uranium when determining which target material to utilize.

Prior to making a final decision on the target material to use for the ADS design, the previous work performed in this area by Liu was analyzed.[12] Table 2 and Figure 6 show the results from the target material analysis study performed by Liu.

Table 2: Target Material Neutron Production Efficiency Results[12]

		Electron Accelerator Energy (MeV)					
	Target Materials	100	200	400	600	800	1000
Neutron Generation per Electron	Tantalum (Ta)	3.141E-02	6.547E-02	1.315E-01	1.963E-01	2.673E-01	3.298E-01
	Tungsten (W)	3.626E-02	7.325E-02	1.470E-01	2.153E-01	2.906E-01	3.574E-01
	Lead (Pb)	3.247E-02	6.510E-02	1.292E-01	1.905E-01	2.478E-01	3.179E-01
	Bismuth (Bi)	3.368E-02	6.680E-02	1.333E-01	1.998E-01	2.599E-01	3.249E-01
	Thorium (Th)	5.790E-02	1.209E-01	2.461E-01	3.679E-01	4.904E-01	6.077E-01
	Uranium (U)	7.05E-02	1.50E-01	3.02E-01	4.51E-01	5.85E-01	7.62E-01

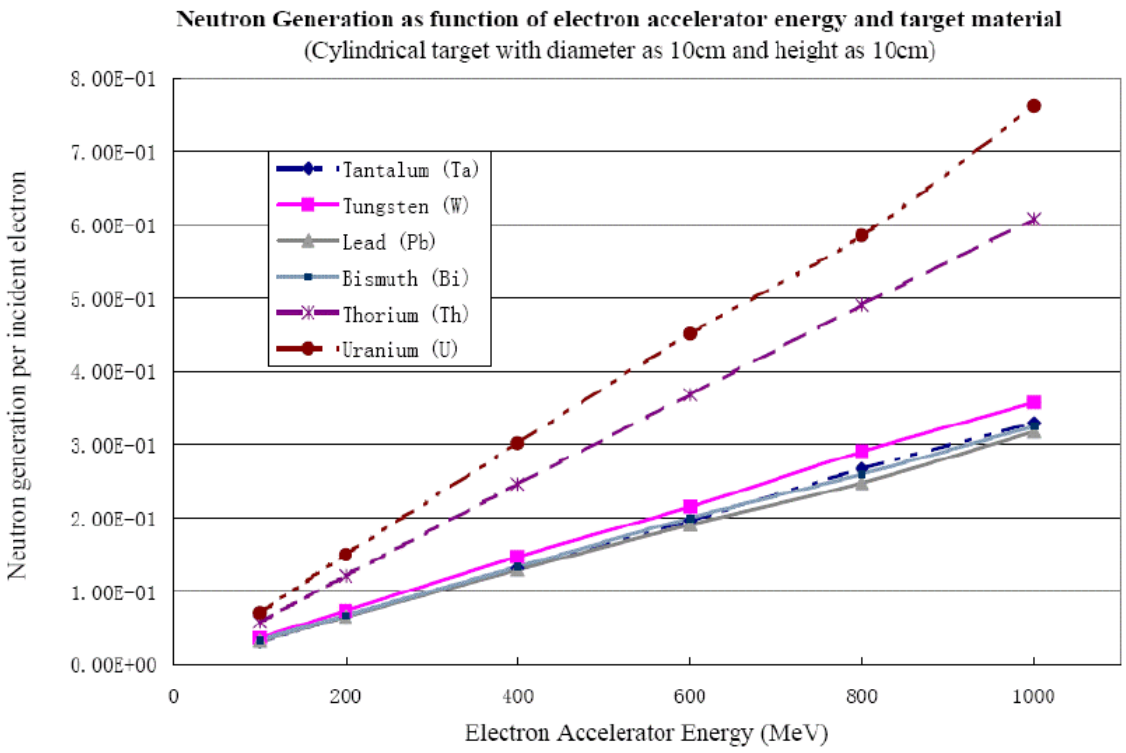

Figure 6: Target Material Neutron Production Efficiency Results[12]

From Table 2 and Figure 6 the same two trends observed in Figure 5 can be seen. For all of the materials, a dependence of neutron conversion efficiency on electron beam energy is shown between 100 and 1000MeV. Once again, uranium has the highest neutron conversion efficiency of all the material tested. However, one other material, Thorium, which was not studied by Yodersmith, also had a high neutron conversion efficiency compared to the rest of the candidate materials.

After reviewing the results of the target material studies presented above, uranium was shown to be the candidate material most efficient at producing neutrons per incident electron. Thorium, was the second most efficient candidate target material within the energy range of 100-1000MeV. Tungsten, however, was the most efficient target material that would not easily create actinides by capture processes within the target. Liu

utilized uranium in his ADS design to utilize the highest possible neutron efficiency and Yodersmith utilized tungsten in an attempt to combined high neutron production efficiency without any risk of TRU production within the target.

The electron ADS design used in this study will utilize a uranium target. The target size that maximizes neutron production is another key aspect when designing the target for use in an ADS. A cylindrical target was used in this study and the data used for neutron conversion efficiencies from other studies also utilized a cylindrical target. Table 3 shows the results from Liu's report for various sizes of uranium targets exposed to a flux of 10,000 1 GeV electrons focused in a 1cm diameter beam for a uranium target.[12]

Table 3: Neutron Yield per Incident Electron for Various Target Sizes[12]

Target Thickness (cm)	Target Diameter (cm)						
	1	3	5	10	20	30	40
1	1.251E-01	1.219E-01	1.254E-01	1.252E-01	1.259E-01	1.261E-01	1.261E-01
2	3.589E-01	4.284E-01	4.066E-01	4.076E-01	4.085E-01	4.092E-01	4.095E-01
3	4.628E-01	5.651E-01	6.073E-01	6.019E-01	6.019E-01	6.037E-01	6.043E-01
4	4.959E-01	6.447E-01	6.758E-01	6.753E-01	6.836E-01	6.871E-01	6.859E-01
5	5.057E-01	6.826E-01	7.020E-01	7.194E-01	7.250E-01	7.306E-01	7.313E-01
8	5.153E-01	7.060E-01	7.243E-01	7.472E-01	7.260E-01	7.158E-01	7.226E-01
10	5.148E-01	7.073E-01	7.220E-01	7.617E-01	7.528E-01	7.426E-01	7.428E-01
13	5.141E-01	7.033E-01	7.243E-01	7.544E-01	7.467E-01	7.387E-01	7.358E-01
16	5.142E-01	7.029E-01	7.238E-01	7.534E-01	7.416E-01	7.336E-01	7.232E-01
20	5.142E-01	7.029E-01	7.234E-01	7.535E-01	7.398E-01	7.165E-01	6.981E-01
30	5.142E-01	7.029E-01	7.233E-01	7.543E-01	7.394E-01	7.048E-01	6.824E-01
40	5.142E-01	7.029E-01	7.233E-01	7.543E-01	7.393E-01	7.042E-01	6.782E-01

The results shown in Table 3 indicate higher neutron yields can be accomplished by increasing the size of the target up to a point. However, one of the benefits of the electron ADS over a proton ADS is the possibility of a smaller target; therefore, the target size providing the optimum neutron conversion efficiency at a reasonable size was

chosen for this study. After 10-13 cm of thickness, the neutrons escaping the target do not increase with increasing thickness and in some cases actually decrease. Therefore, a target thickness of 10 cm is the optimum target size for an electron ADS design. The maximum neutron flux escaping the outer surface of the target with a thickness of 10 cm occurred with a diameter of 10 cm. However, the neutron flux for target with diameters 3 and 5 cm are comparable to the 10 cm diameter target. Therefore, if a smaller target is desired, targets with diameters in the range of 3-5cm would produce neutron fluxes on the same order as much larger targets. Once the target material has been chosen, the target size can be more accurately determined.

2.2 ACCELERATOR BEAM

Previous studies have indicated that there is a relationship between the electron beam energy and the neutron production efficiency of the materials. The correlation between the neutron conversion efficiency and accelerator beam energy appears to be linear; however, this does not necessarily mean using a higher accelerator energy is the best option. Instead, an analysis needed to be performed to determine if more neutrons could be produced for a given overall accelerator power level by using a higher energy beam and therefore utilizing the higher neutron conversion efficiency or to use a lower energy beam with a higher flux of incoming electrons to offset the lower neutron production efficiency. Therefore, the relationship between the neutron production efficiency (neutrons/electron) and the electron beam energy (MeV) needed to be quantified. For a uranium target, the neutrons produced per electron per accelerator energy, or neutrons produced per unit of accelerator power, increases with higher accelerator energies in the range of 100-300 MeV and then between 300-1000 MeV the

value is constant.[10] Therefore, anywhere between 300-1000 MeV, for a given accelerator power, the same number of neutrons are produced by either utilizing a higher beam current at low energies or the higher conversion ratio at high energies. Since, the number of neutrons produced per electron per accelerator energy is constant for electron accelerator systems between the energies of 300-1000MeV other factors besides neutron production must be investigated to determine the optimum accelerator energy for use in a transmutation facility.

A related factor of interest in determining the accelerator beam energy is the technical feasibility of the selected beam energy. The presence of facilities with experience for specific electron accelerator beam energies needs to be verified. A list of some of the high energy electron accelerators operating around the world is given in Table 4.

Table 4: High Energy Electron Accelerators

Accelerator	Location	Electron Energy Range (Mev)
ELSA[13]	Germany	500-3500
Bates Linear Accelerator[14]	USA	300-1100
CEBAF[15]	USA	Up to 6000
MAMI[16]	Germany	Up to 1508

From Table 4 it is clear electron accelerators with energies up to and beyond 1,000MeV have been built and operated. Currently there are not many electron accelerators operating at 1,000MeV. As deployment of an ADS is considered to be decades in the future[7], it is assumed electron accelerators with energies up to 1,000MeV and higher will become more feasible by the time an ADS is deployed.

The majority of this thesis deals with a study on the effect of loading patterns on the k_{eff} and peaking within a single target fast flux electron ADS. Use of multiple targets within the electron ADS in an attempt to achieve more acceptable power peaking factors within the reactor core is also investigated. Therefore, the ability to provide an electron beam from the accelerator facility to multiple targets must be considered. There are two possible methods for creating multiple electron beams from the accelerator facility for use within the ADS. The first method would be to utilize multiple accelerators. The use of multiple accelerators is feasible; however, the second method where the beam from one accelerator is split into multiple beams would be a more capital cost efficient method. Accelerator beam splitting is performed at many currently operating accelerators used for experiments. For example, CEBAF the accelerator with the highest energy electron beam listed in Table 4 can split the beam into two or three separate experiment halls with the beam current being divided among the targets.[17]

2.3 NEUTRON SPECTRUM

The third component in an ADS is the subcritical core which multiplies the neutrons from the target. The multiplied neutron flux is used to transmute the waste within the reactor core. The first major decision for the design of the subcritical core for an ADS is whether to use a fast or thermal neutron flux within the core. ^{90}Tc and ^{129}I, the fission products of most concern in SNF waste cannot be effectively transmuted within a fast reactor flux. Therefore, if transmutation of these fission products is a high priority, a thermal reactor design must be used for the ADS subcritical core. However, if transmutation of the TRUs in SNF are the major goal of the ADS, then the cross-sections of the TRUs in thermal and fast flux reactors needs to be examined. As discussed above,

neutron capture for TRUs does not easily result in stable isotopes. Therefore, the goal of the ADS is to fission the TRUs. To ensure neutron economy within the ADS, the capture to fission ratio of the TRUs becomes the most important factor. Figure 7-Figure 19 show the capture and fission cross-sections of ^{237}Np, ^{238}Pu, ^{239}Pu, ^{240}Pu, ^{241}Pu, ^{242}Pu, ^{241}Am, ^{242m}Am, ^{243}Am, ^{244}Cm, ^{245}Cm, ^{246}Cm, and ^{247}Cm for energies up to 20 MeV. These plots were produced using ENDFPLOT II[18] and the MCNP library. The cross-sections of other TRUs were also studied but only the TRUs that were eventually used in the final design are provided here.

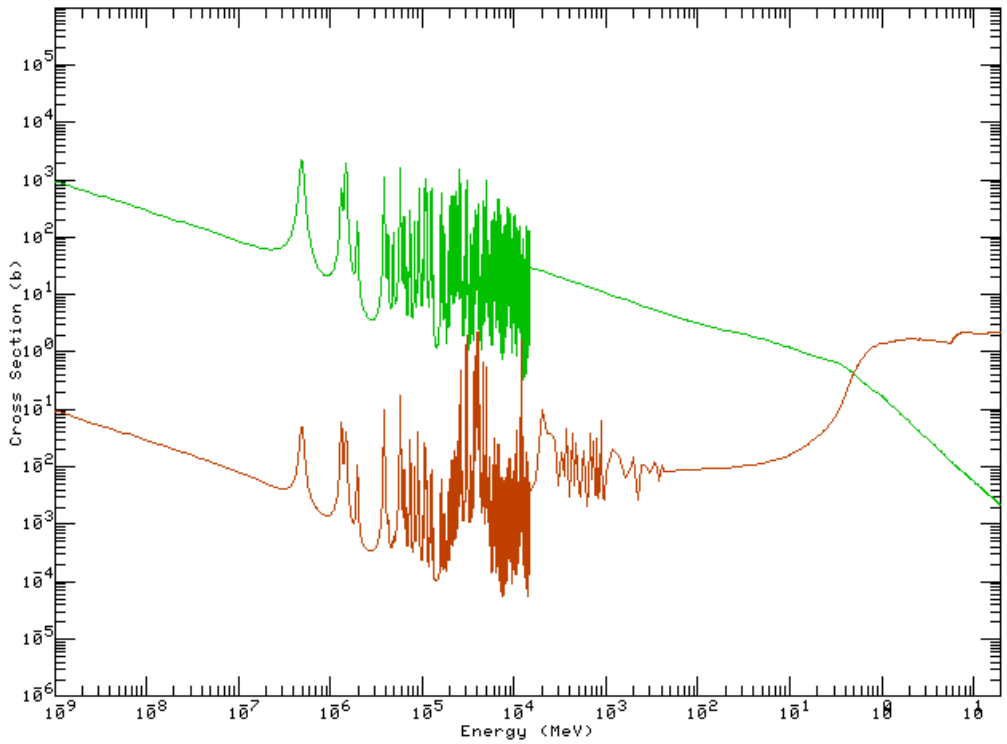

Figure 7: Np-237 Cross Sections (Fission-Brown; Capture-Green)

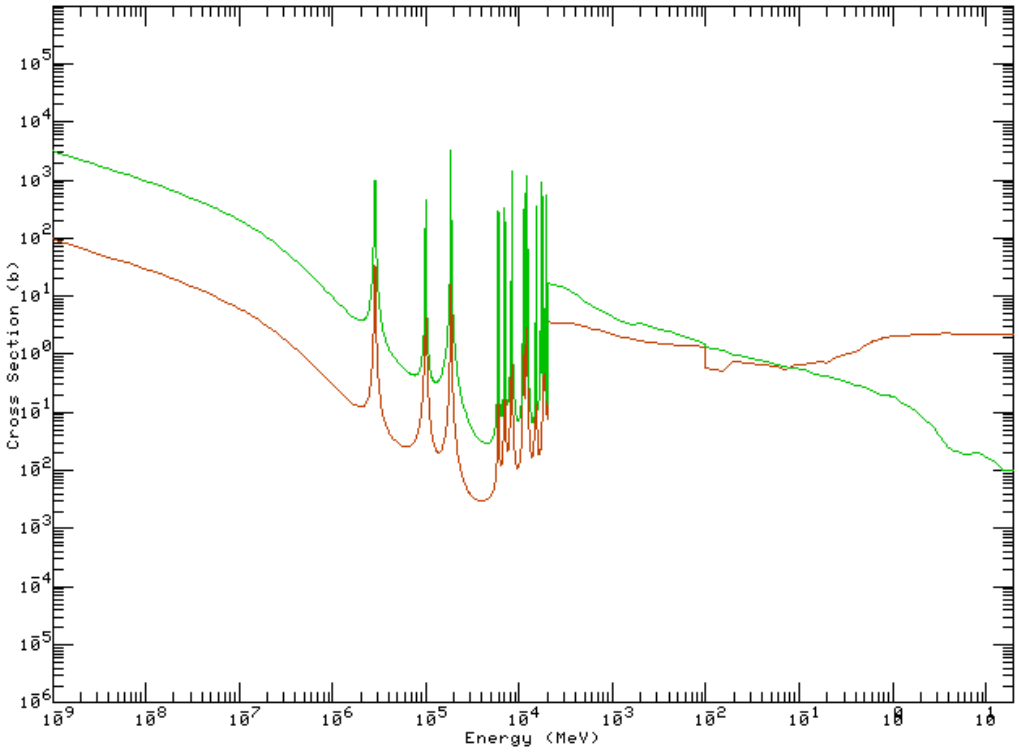

Figure 8: Pu-238 Cross Sections (Fission-Brown; Capture-Green)

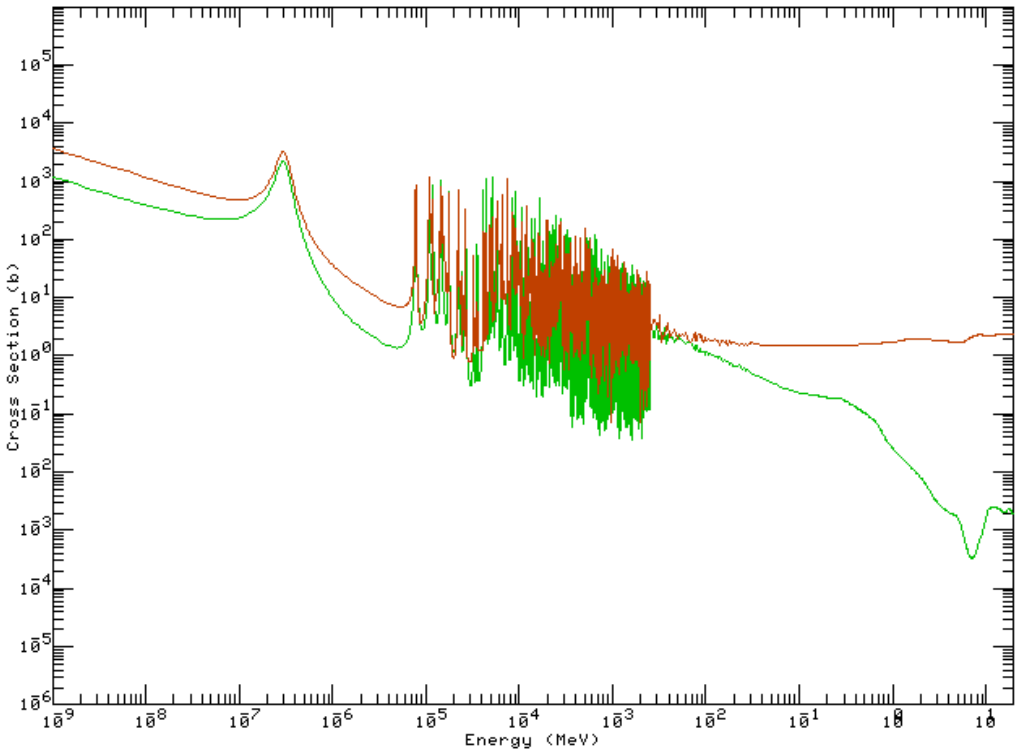

Figure 9: Pu-239 Cross Sections (Fission-Brown; Capture-Green)

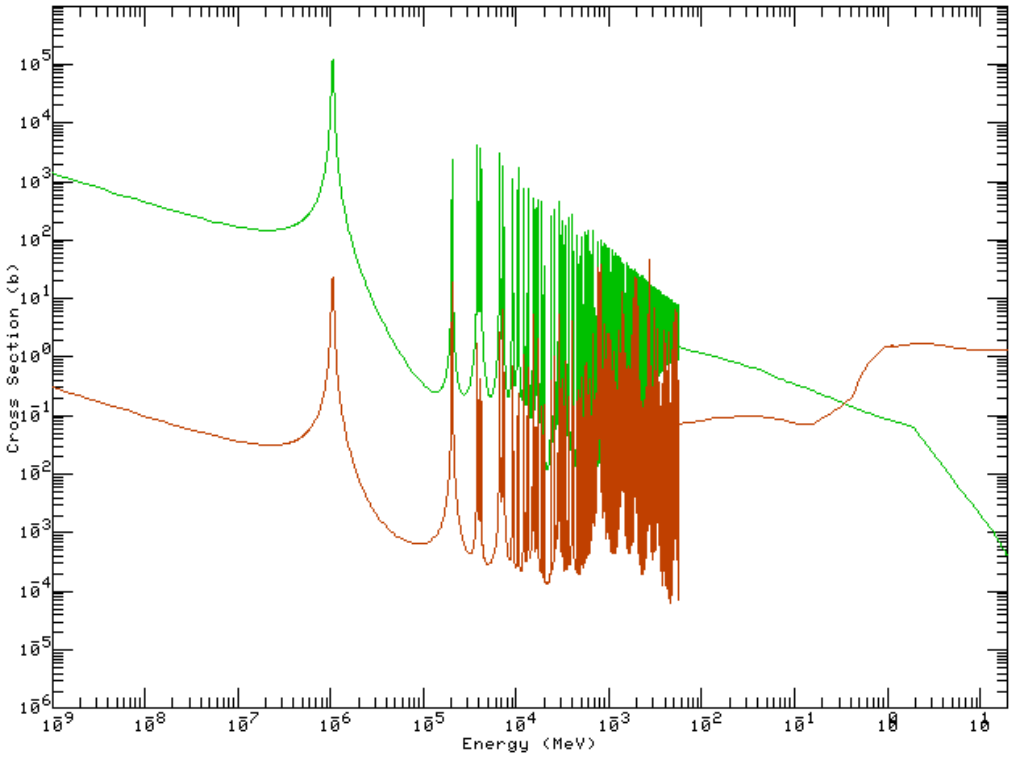

Figure 10: Pu-240 Cross Sections (Fission-Brown; Capture-Green)

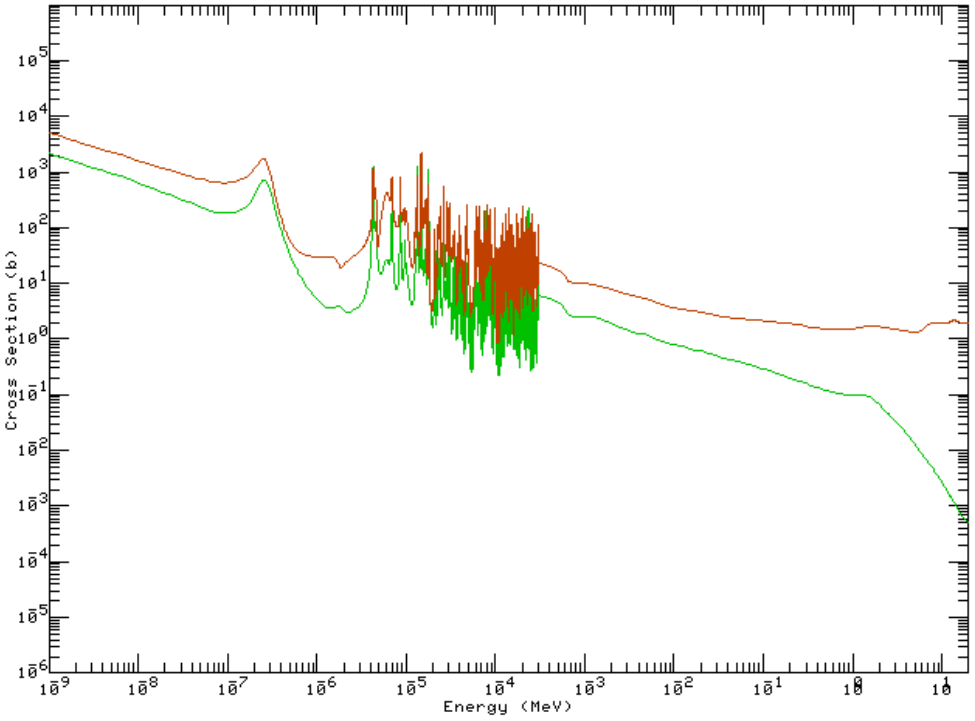

Figure 11: Pu-241 Cross Sections (Fission-Brown; Capture-Green)

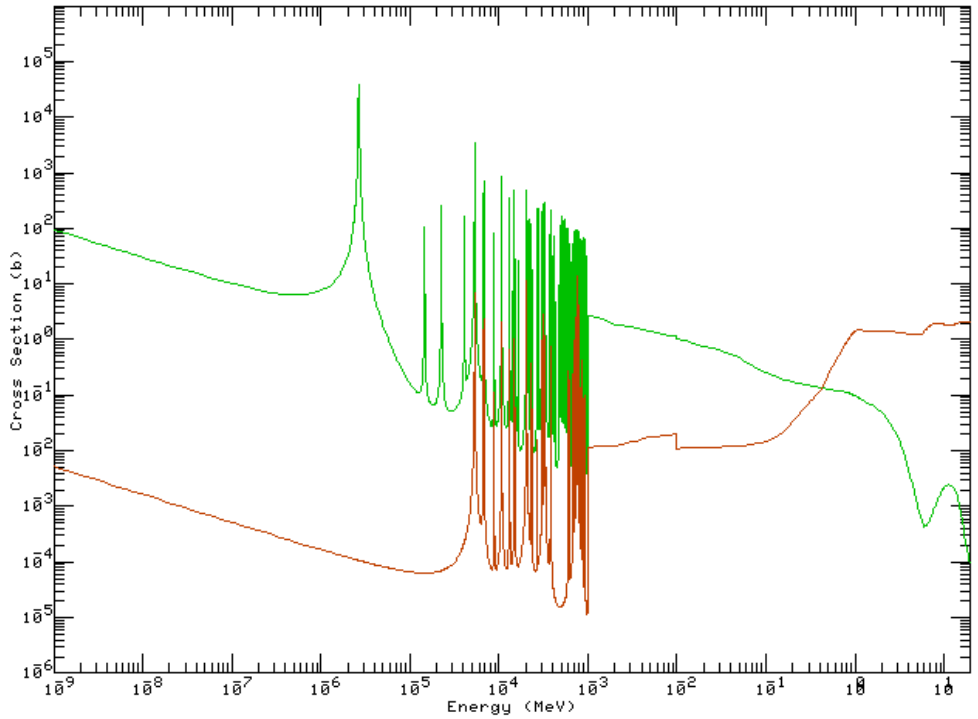

Figure 12: Pu-242 Cross Sections (Fission-Brown; Capture-Green)

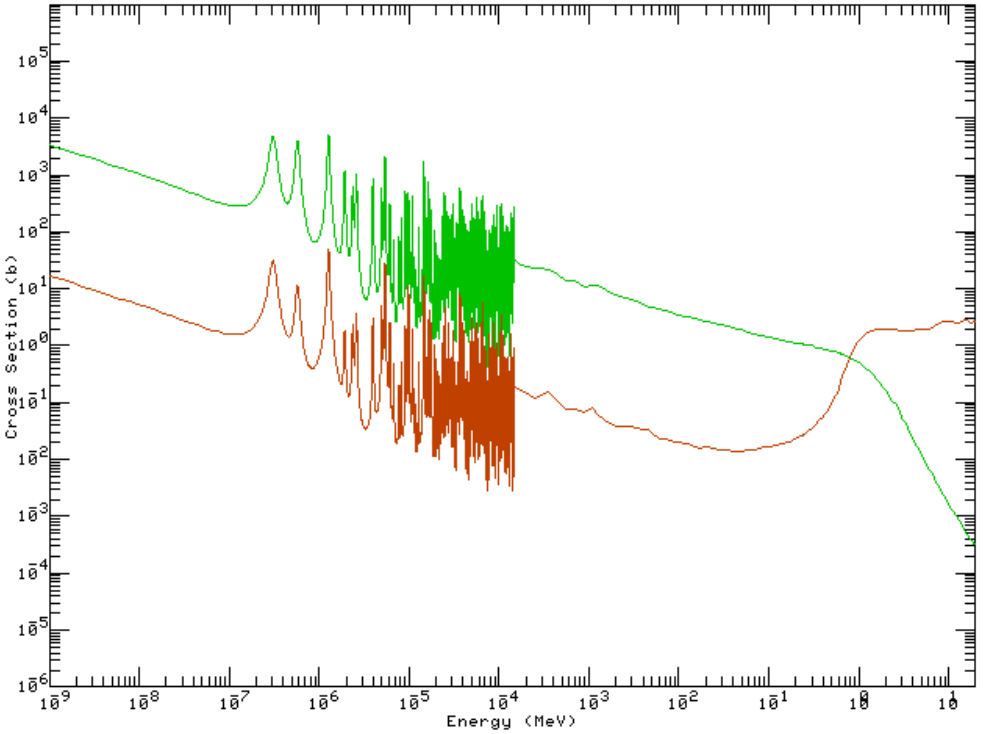

Figure 13: Am-241 Cross Sections (Fission-Brown; Capture-Green)

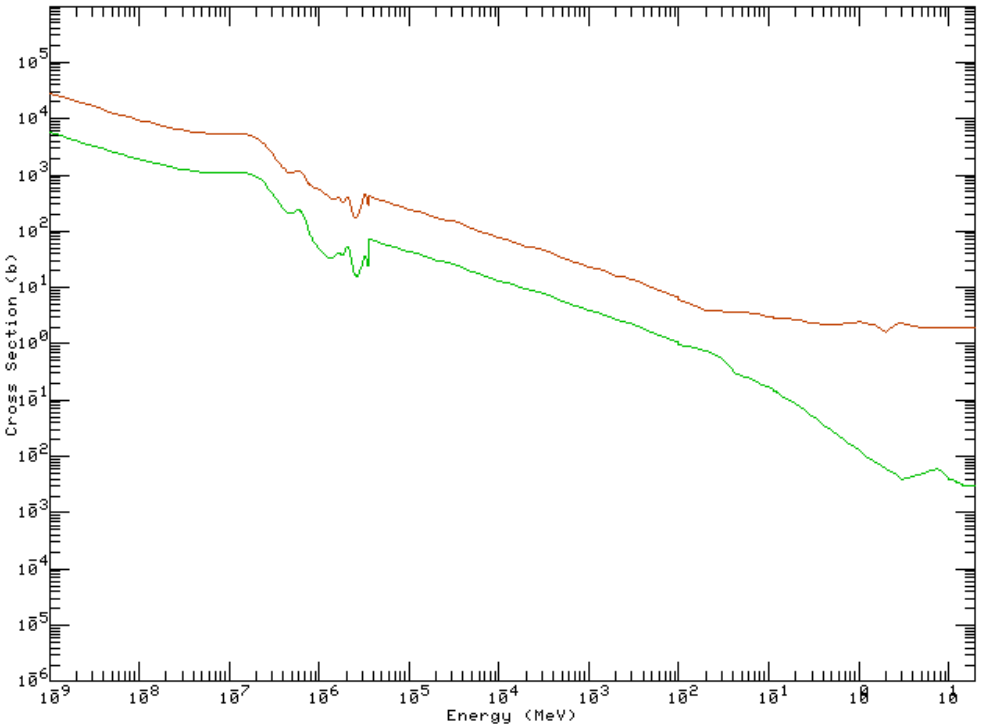

Figure 14: Am-242m Cross Sections (Fission-Brown; Capture-Green)

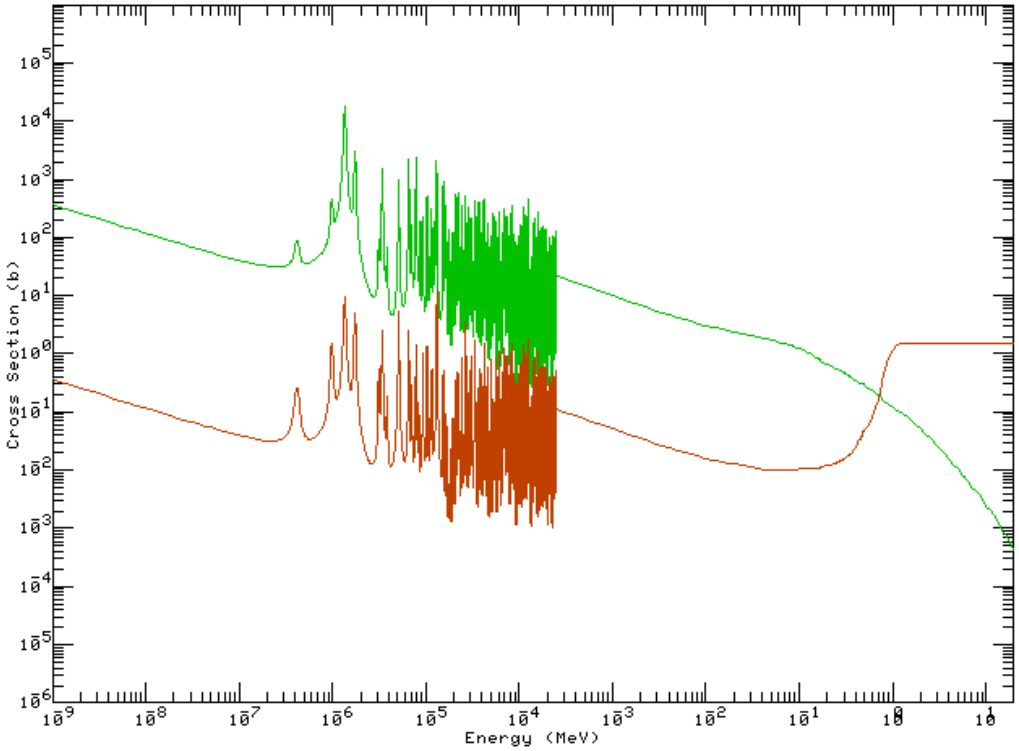

Figure 15: Am-243 Cross Sections (Fission-Brown; Capture-Green)

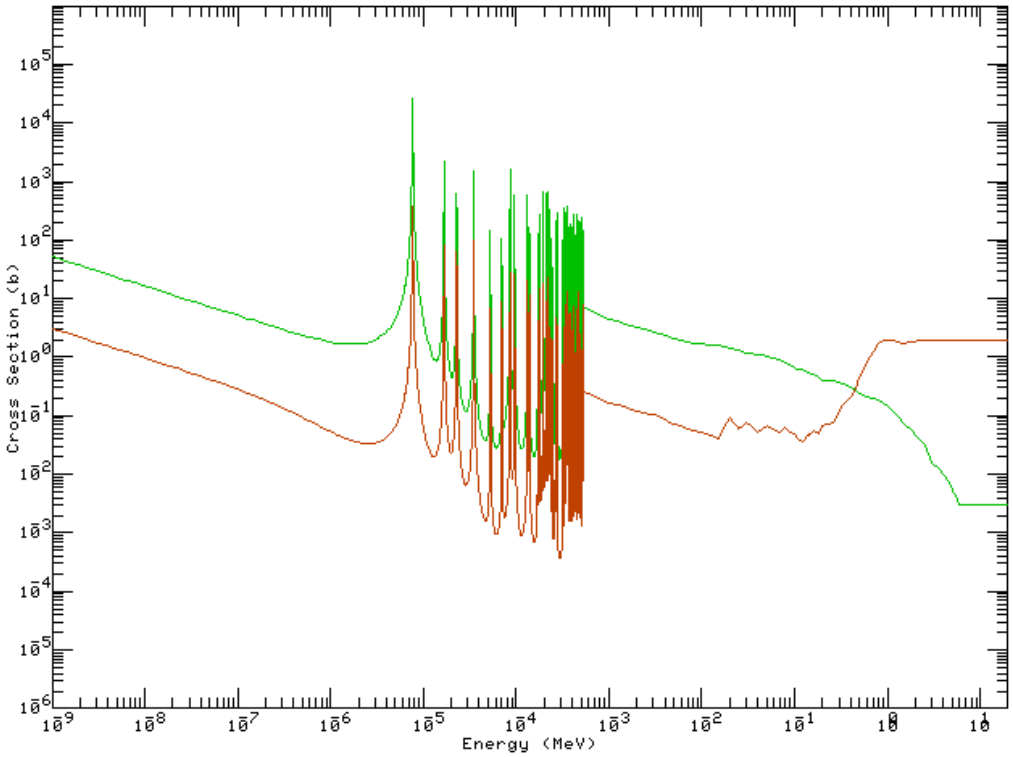

Figure 16: Cm-244 Cross Sections (Fission-Brown; Capture-Green)

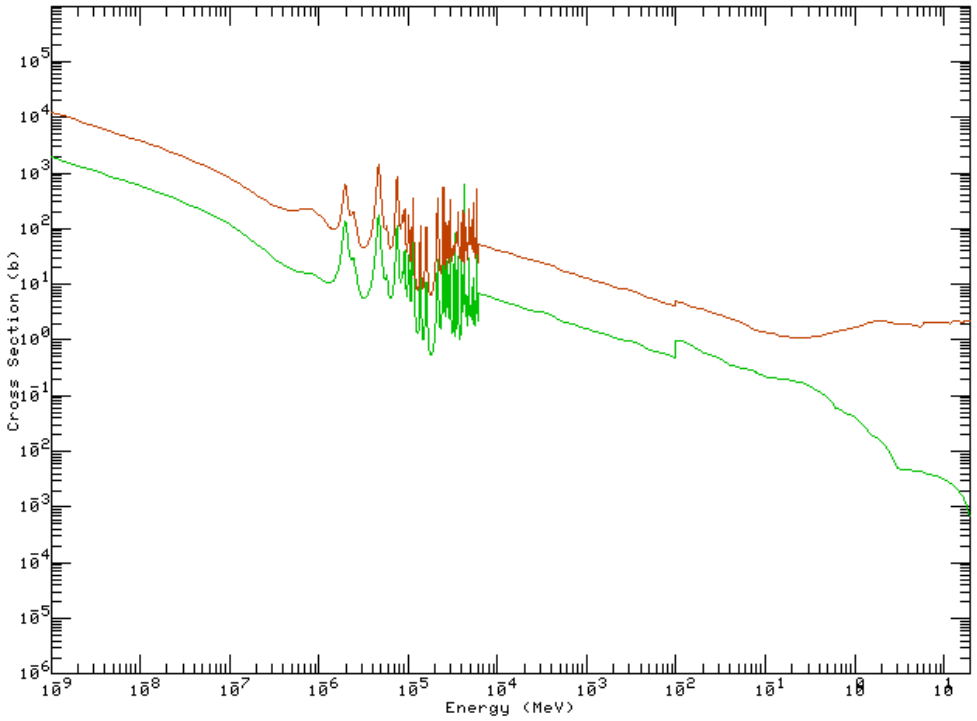

Figure 17: Cm-245 Cross Sections (Fission-Brown; Capture-Green)

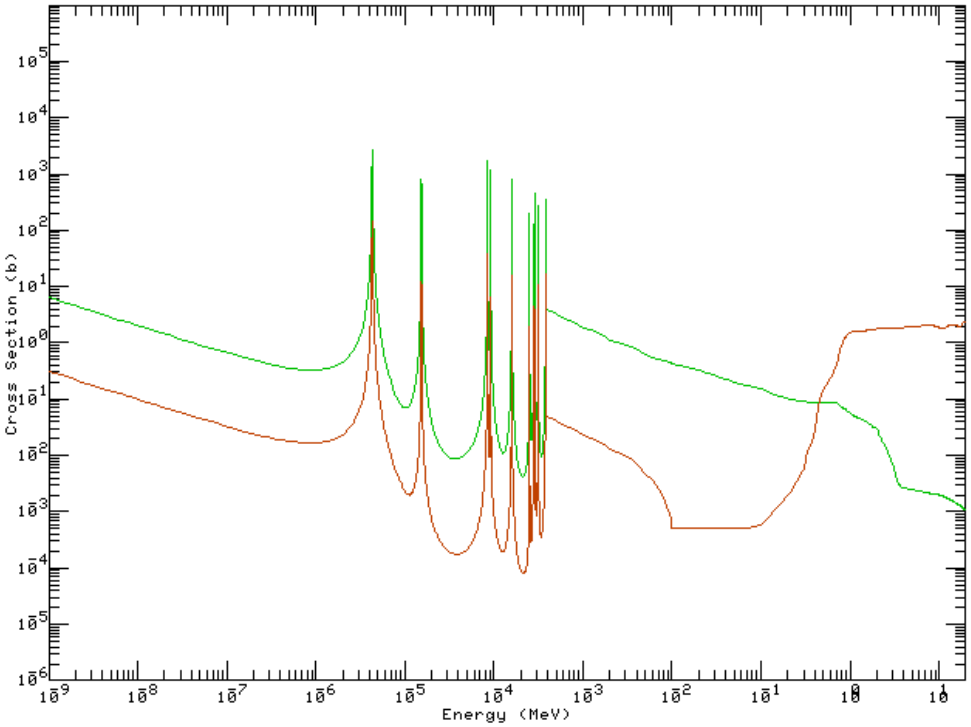

Figure 18: Cm-246 Cross Sections (Fission-Brown; Capture-Green)

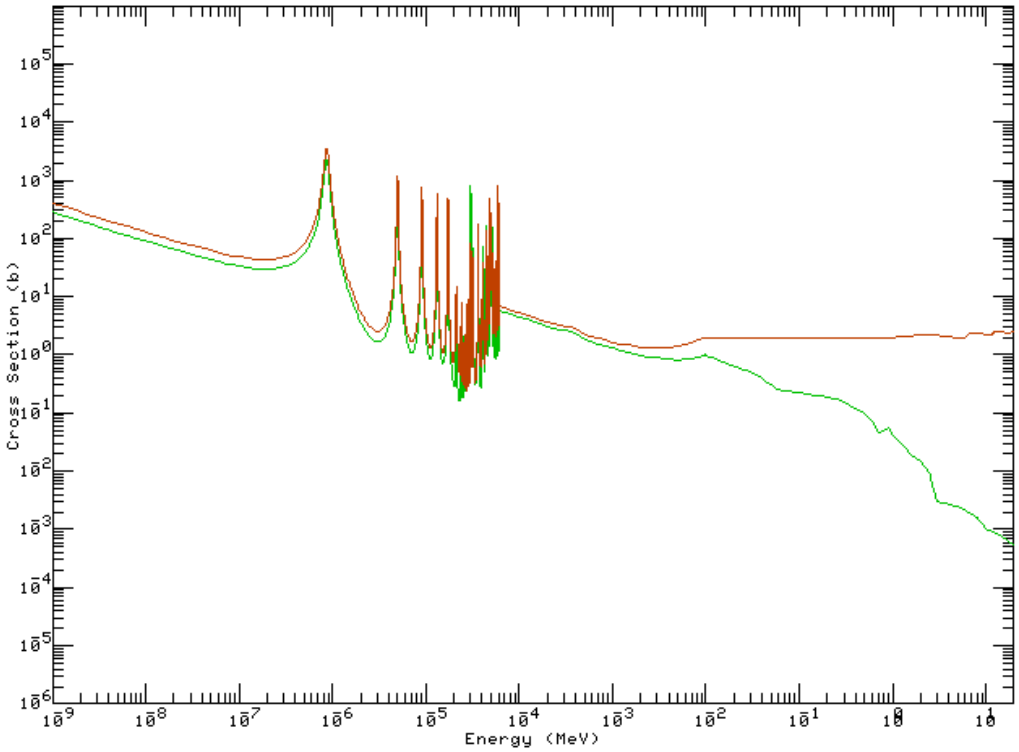

Figure 19: Cm-247 Cross Sections (Fission-Brown; Capture-Green)

Figure 7-Figure 19 show for all TRUs used in the final design the fission cross-section is higher than the capture cross-section above ~0.5-0.7MeV. Five of the TRUs shown above have higher fission than capture cross-sections across the entire energy range, except possibly at some resonance locations. Therefore, when considering the higher fission to capture cross-section of the TRUs as the main design criteria, a fast reactor flux is the best design for the sub-critical core when the transmutation of the TRUs present in SNF is the primary concern.

2.4 FUEL MATERIALS

All LWR power reactors currently operating in the US utilize UO_2 as the fuel form. UO_2 is a solid ceramic with a large experience base for reactor operations and design. However, the fuel for an ADS will not utilize uranium because more waste would be produced during operations. Operating and designing reactors using TRU fuel does not have a large experience base with any particular fuel form; therefore, the fuel form used for an ADS design is more open-ended than choosing a fuel form for a traditional uranium fueled power reactor. ADS fuel can be in either a solid or liquid form.

The use of liquid fuel in nuclear reactors has been briefly studied at various times. However, most of these experiments have dealt with thermal neutron spectra. Therefore, the experience base for a fast spectrum liquid fuel reactor is very limited when compared to solid fuel reactors. A possible benefit of using a liquid fueled reactor for an ADS is online reprocessing of the fuel. If online reprocessing of the fuel is possible, then there would not be a need to fluctuate the accelerator beam current to maintain k_{eff} since the fuel could be constantly processed to maintain the proper ratio of fuel materials necessary

for criticality. The most prominent liquid fueled reactor experiment in the US was the Molten Salt Reactor (MSR) operated at Oak Ridge National Laboratory between 1950 and 1976. During the MSR experiment, many problems associated with a molten salt reactor were identified including corrosion/noble metal plating, reactions between the molten salt and water working fluid of a Rankine power cycle, etc. However, some of these problems may be alleviated by technologies developed in the 30+ years since the MSR was shutdown.[19] Even with these new technologies for a molten salt reactor, liquid fueled reactors are generally more likely to be considered for use in a thermal spectrum ADS.[4]

Compared to a liquid fueled thermal reactor design, almost all designs of fast reactors have utilized a solid fuel form. The use of solid fuels is considered more compatible with a fast spectrum reactor. The use of solid fuels also has a much larger experience base and has been under continuous research and development throughout the world in fast reactors. Metal alloy fuel is also compatible with the pyrochemical reprocessing technique developed by Argonne National Laboratory for use in the proposed ADS fuel cycle.[4] Table 5 provides a comparison of using either a solid or liquid fuel form in the fast spectrum ADS design.

Table 5: Comparison of Solid and Liquid Fuel Forms for a Fast Spectrum ADS[20]

Solid Fuel Form	Liquid Fuel Form
Compatible with pyrochemical reprocessing technique	Possibility of online reprocessing capability
Suitable for fast spectrum ADS	Typically used in thermal spectra
Larger experience base	Almost non-existent experience base for fast spectrum reactors
	Issues identified during MSR experiment may be insurmountable

Given the information given above and summarized in Table 5, the design for a fast spectrum ADS would most likely utilize a solid fuel form. Some of the possible solid fuel types are metals fuels (usually alloys), nitride pellets, dispersion fuels, or TRISO coated fuel particles. Table 6 lists the advantages and disadvantages possible by using a metal alloy fuel in an ADS environment.

Table 6: Advantages and Disadvantages of Metal Alloy Fuels[20]

Advantages	Disadvantages
High fissile atom density	Little to no experience with non-fertile compositions
High thermal conductivity	Fuel-cladding chemical interaction (or interdiffusion)
Low heat capacity	Loss of volatile americium during fabrication
High thermal expansion	Limitations to fuel temperature to avoid melting (not a restrictive criterion in EBR-II experience)
Potentially simple fabrication	
Established experience base for U-bearing fuels (EBR-II, IFR)	

From Table 6 there are currently four identifiable disadvantages to using a metal alloy fuel for the ADS design. The first disadvantage listed is the low experience base for metal alloy fuels with non-fertile compositions. However, from Table 7-Table 9 we also see none of the four candidate fuel types have a large experience base for non-fertile fuels. TRISO coated particles have the largest experience base but it is still not large enough to place it ahead of the other candidates. One of the other disadvantages listed for metal alloy fuel is the limitations on fuel temperatures required to avoid melting. However, this restriction was not a factor in the design of a previous metal alloy fueled

reactor, the EBR-II.[20] One concern with the limit on fuel temperatures is the higher peaking factors in an ADS core than other core designs such as the EBR-II.

Most of the advantages for a metal alloy fuel type concern safety margins within a reactor. However, the metal alloy fuel type is the only fuel type with a relatively simple fabrication process developed. This is a large benefit over the other possible fuel types. Since the goal of an ADS design is to fit into the fuel cycle such that nuclear power maintains its economic viability, low cost of fuel fabrication is essential. In a solid fueled ADS system, the fuel will most likely be reprocessed several times to be returned to the reactor; therefore, cheap fabrication techniques are highly beneficial. Table 7 lists the advantages and disadvantages of nitride pellet fuel.

Table 7: Advantages and Disadvantages of Nitride Pellet Fuels[20]

Advantages	Disadvantages
High fissile atom density	Little to no experience with non-fertile compositions
High thermal conductivity	Small irradiation performance database for higher burnup and little or no transient testing experience
Relatively high fuel temperatures allowable	N14(n,p)C14 reaction
Potential for reduced volatility of americium during fabrication	Some issues with fragmentation of (U,Pu)N
Chemical compatibility with sodium and lead-bismuth eutectic	Fabrication using powders
Some experience base for U-bearing fuels (LMFBR, SP-1000)	
Considerable interest in Europe and Asia	

In Table 7, the disadvantage of a low level of experience with non-fertile compositions of the fuel type is listed again. However, unlike metal alloy fuels, nitride fuel pellets require fabrication using powders which is a disadvantage. Nitride fuel also must worry about $^{14}N(n,p)^{14}C$ reactions when exposed to the neutron flux within a reactor

core. The main benefit of nitride fuels over metal alloys is the possibility of higher fuel temperatures. When considering the disadvantages versus the advantages of using a nitride pellet fuel form within the ADS design, metal alloy fuels were considered the better choice. However, as shown in Table 8, using a dispersion fuel may provide benefits over metal alloy fuels not provided by nitride pellets.

Table 8: Advantages and Disadvantages of Dispersion Fuels[20]

Advantages	Disadvantages
High-burnup potential	Little to no experience with non-fertile compositions or fuel particles of the type proposed
High thermal conductivity	Low fissile density
Relatively high fuel temperatures allowable for nitride	N14(n,p)C14 reaction for nitride
Potential for reduced volatility of americium during fabrication of nitride	Possible temperature limitations for metallic dispersion
Chemical compatibility with sodium	Chemical compatibility with lead-bismuth eutectic for some matrix metals
Some experience base for U-bearing fuels	Fabrication using powders

Table 8 shows dispersion fuels have many of the same limitation as metal alloy fuels. The presence of $^{14}N(n,p)^{14}C$ reactions promotes the use of metal dispersion fuels over nitride dispersion fuels. Therefore, the temperature limits of the fuel are similar between the metal dispersion and metal alloy fuels. Metal dispersion fuels have the disadvantage of fabrication requiring powders; however, it has a major advantage over metal alloy fuels. The primary advantage of metal dispersion fuels over metal alloy fuels is the possibility of higher burnup limits. High burnup limits are important in an ADS design. With higher burnup limits the waste can be transmuted in a given cycle of the ADS to a higher degree. The result is longer cycles for the ADS which reduce the number of fabrications required, thereby limiting the effect of the fabrication technique

advantage present in metal alloy fuels. In order to make the decision between using a metal alloy or metal dispersion fuel in the ADS a more thorough examination of the burnup differences in the two fuel types must be made. However, before examining this factor, a comparison with TRISO coated fuel particles is made. The aspects of using TRISO coated fuel particles is listed in Table 9.

Table 9: Advantages and Disadvantages of TRISO Coated Fuels[20]

Advantages	Disadvantages
High-burnup potential	Small experience base with non-fertile compositions
High fuel temperatures allowable for nitride	Reliability of fuel particles in fast spectrum uncertain, at best
Good experience base for U-bearing fuels, and a small favorable experience base for a non-fertile oxide (PuO_2)	Impact of multiple valence states of TRU oxides on fabrication of fuel kernels
Some interest in non-fertile compositions for Pu disposition in Russia	Fabrication using powders

From Table 9, the TRISO coated particles have some different advantages and disadvantages from the metal alloy or dispersion fuel types. TRISO coated fuel particles do have high burnup limits as a main benefit. However, the major disadvantage of the TRISO fuel particles is the fabrication of the fuel kernels when using TRUs. The fabrication of TRISO fuel also relies on powders and these two disadvantages have a large impact when designing an ADS system with TRU fuel where multiple fabrications may be required. Fabrication of TRISO fuel is already a major technical hurdle and the addition of complication form TRU oxides during the process merely increases the difficulty. Since the fabrication process for TRISO particles appears to be the main technical 'show-stopper' and multiple fabrications will be required in the ADS fuel cycle, the potential cost increase for using TRISO particles appear to outweigh its benefits.

Therefore, the fuel type used in the fast spectrum ADS design is narrowed down to metal alloy and metal dispersion fuels.

The major benefit of metal dispersion fuels over metal alloy fuels listed above is the possibility of higher burnup limits which may overcome the disadvantage in the fabrication process of metal dispersion fuels. Experimental data concerning the burnup limits of metal alloy fuels versus metal dispersion fuels is practically non-existent. However, some simulation data does exist which compares the burnup capabilities of dispersion and ally fuels. Before analyzing the burnup data for the two fuel types, a note regarding the helium generation during the transmutation of ^{241}Am must be made. During the transmutation of ^{241}Am, the americium can capture a neutron and become ^{242}Cm after beta decay. The ^{242}Cm then alpha decays to ^{238}Pu, thereby producing helium within the fuel structure. The effect of the He generation within metal dispersion fuels has a much greater impact than He generation in metal alloy fuels. The values of cladding strain as a function of burnup are nearly identical in metal alloy fuel with and without He generation effects. However, in dispersion fuel the cladding strain at a burnup level of 30a/o is 2.85% without He generation effects and 3.3% with He generation effects. Comparing these numbers with the 3.01% cladding strain in metal alloy fuel with 30a/o burnup reveals that the burnup limit of the dispersion fuel may be lower or higher than alloy fuel depending on the He generation effects.[21] If metal dispersion fuels cannot provide higher burnup levels than metal alloy fuel, the fabrication advantage of the metal alloy fuel takes precedence. ^{241}Am accounts for over 6% of the TRUs present by mass in the ADS fuel. Therefore, the He generation effect cannot be ignored and the possibility of higher burnup limits for metal dispersion fuel is lowered.

2.5 CORE COOLANT

The primary candidates for coolant in a fast reactor are lead, lead-bismuth eutectic, sodium, and helium. The first three choices are liquid metals while helium would be a gas cooled reactor. To decide which coolant option to utilize in the reactor design, the benefits and disadvantages of each option were analyzed. In a fast reactor, the coolant should have a small capture cross section, high scattering cross section, low energy transfer per collision to reduce moderation, and a larger single phase operating range.[22] All of the above coolant choices meet these requirements to varying degrees and exhibit other beneficial qualities.

The most unique coolant choice listed above is helium which would result in a gas cooled reactor design for the electron ADS. The design of gas cooled reactors has been promoted for various reasons; however, the progress in designing a helium cooled reactor is much farther behind than either a lead, lead alloy, or sodium cooled reactor. Lead and sodium cooled reactors have been operated before, particularly in the United States and Russia. One possible benefit of using an electron ADS over a proton ADS is that electron accelerators are currently more developed, and therefore more stable, which is highly beneficial in a reactor environment. Therefore, the electron ADS design should attempt to utilize characteristics that are as far along in development as possible to allow for the earliest possible deployment date of the system. When considering this, the use of helium as a coolant within the electron ADS design is not considered beneficial due to its low level of experience and knowledge base around the world when compared with the other coolant choices.

Lead-bismuth eutectic (LBE) is a lead bismuth alloy with the proportion of lead to bismuth which has the lowest melting point of any combination of the two components. For a lead-bismuth alloy the eutectic occurs with 55.5w/o bismuth and 45.5w/o lead. Lead has a melting point of 327.4^{o}C and bismuth's melting point is 271^{o}C; however, LBE has a much lower melting point at 123.5^{o}C. The low melting point of LBE is beneficial in a fast reactor design which utilizes high operating temperatures but will also experience lower temperatures during shutdown. A low melting temperature decreases the need for special equipment for the coolant to be kept in or changed into the liquid phase at shutdown temperatures. The boiling temperature of LBE is very high at 1670^{o}C satisfying the large single phase operating range requirement for the coolant. Having a high boiling temperature reduces the need to consider reactivity effects from voids in the coolant.[22]

LBE is composed of lead and bismuth which are both elements with high atomic numbers. The heavy atoms LBE is composed of result in a low energy transfer per collision between the coolant and neutrons within the core. The low energy transfer rate results in a harder energy spectrum within the ADS which utilizes the higher fission to capture cross section ratios of the TRUs at higher energies. LBE also has a low capture cross section which is important in an electron ADS with its lower neutron productions efficiency in the target when compared with the proton ADS. LBE has other benefits such as a low volume change up solidification, a high level of gamma shielding and fission product retention in case of core accidents.[7]

The neutronics performance and operating temperature range of LBE suggest it would be highly compatible with the electron ADS design. However, there are some

disadvantages to using LBE within the design. LBE is highly corrosive and can dissolve steels that may be utilized in the core construction. LBE's operating experience base in the United States is non-existent. However, in Russia there is a much larger experience base with lead and LBE coolants. In Russia, there has also been progress in developing a method to control the corrosiveness of LBE as a coolant. Oxygen is introduced to the system allowing for a protective oxide coat to develop on the core structures. The process is still relatively new and very delicate at this point in its development. Therefore, the availability of the method in the near future for an ADS deployment should not be assumed.[7]

The second disadvantage of using LBE as the coolant in an ADS design is the production of radioactive ^{210}Po within the coolant when exposed to a neutron flux. The ^{209}Bi within the LBE coolant becomes ^{210}Bi after a neutron capture. ^{210}Bi then captures a neutron and after a beta emission becomes ^{210}Po, which emits a 5.1MeV alpha particles with a half-life of 138.3 days. ^{210}Po can be especially harmful during a leakage accident because it disperses quickly in a given volume of space.[22]

The coolant choice that can be most directly compared to using LBE is using a pure lead coolant. Using lead as the coolant would maintain some of the benefits of LBE such as the hard neutron spectrum and beneficial cross sections allowing for low neutron leakages within the core while still minimizing any softening of the neutron spectrum. Using a pure lead coolant also reduces the activation levels of the coolant when compared with LBE. In lead coolant ^{208}Pb can capture a neutron becoming ^{209}Pb which beta decays to ^{209}Bi which as shown above can produce ^{210}Po. However, the level of activation in a lead coolant has been shown to be three orders of magnitude less than LBE Therefore,

lead coolant is able to maintain the beneficial neutronics characteristics of LBE without having the large activation issue associated with LBE.[22]

Using LBE as a coolant does have advantages over using lead. The melting point of pure lead as shown above is 327.4^{o}C. The high melting point of lead posses problems with maintaining the coolant in a liquid phase whenever necessary and would therefore require a more elaborate design to control the temperature of the coolant during shutdown. The corrosion problems that exist for LBE and pure lead are also more pronounced at higher temperatures. A lead coolant would have to be maintained at these higher temperatures more often due to its higher melting temperature, which would further promote the corrosion of core structures exposed to the coolant. The higher melting temperature of lead makes it a less attractive coolant option for the ADS design than LBE. An ADS will be a first time endeavor and uncertainties such as corrosion problems would need to be minimized. Whereas the activation of the coolant is a measurable affect that can be anticipated in the design.

The final coolant option, sodium, has the ability to overcome many of the disadvantages of using LBE, but has numerous disadvantages of its own. Sodium does emit gammas after neutron activation of ^{23}Na; however, the half life of ^{24}Na is 15hrs meaning the post operational concern of dealing with activated coolant is almost non existent. For comparison, calculations determining the cooling down time required for the three coolant types mentioned above in order for the used coolant to be considered acceptable for industrial purposes by the IAEA can be analyzed. For pure sodium coolant the cooling time required is about 7yrs and sodium coolant with activated impurities requires a cooling time of 50-100yrs. A pure lead coolant would require a

cooling time between 10^3 and 10^8yrs and activated LBE coolant would require cooling times beyond any practicable range. Therefore, utilization of sodium as the coolant in an ADS design has a significant advantage over LBE and pure lead when considering the activation of the coolant during operations.[22]

A major disadvantage of using LBE or lead as the coolant in the ADS design was the uncertainties associated with corrosion of core structures in contact with the coolant. Sodium, on the other hand, has large operating experience base using steels as the structural material in the reactor. Sodium and steel have been shown to be compatible in a reactor environment. In a new design such as the ADS, reducing any uncertainties in the design, such as those from corrosion rates, is highly beneficial. In general, the United States has a much larger experience base with using sodium as a coolant for fast reactor designs.

Sodium as a coolant requires significantly lower pumping power than either LBE or lead. The lower required pumping power for a sodium cooled ADS design results in more power back to the grid which is a major concern with the electron ADS compared to the proton ADS. Sodium also has a lower melting temperature than either LBE or lead since its melting point is 97.8^{o}C. However, sodium's boiling temperature is also lower than lead and LBE by 780-840^{o}C. This results in a much smaller overall operating range for utilizing a single phase sodium coolant. However, if the boiling temperature is high enough for normal operations in the ADS design, then the lower melting point is beneficial during shutdown conditions for maintaining the coolant in a single phase at all times.[22]

Sodium does have disadvantages compared to LBE or lead when considering it as a coolant option for a fast spectrum ADS. Sodium does not have as good of neutronics characteristics as the other two liquid metal coolant options. A sodium cooled ADS would experience a greater level of neutron thermalization within the core. This has a negative impact on the fission to capture cross section ratio for the TRUs to be burnt within the design. A sodium cooled reactor cannot be operated in natural convection as easily as a core cooled with LBE or lead. This characteristic of the coolants slightly offsets the lower pumping power requirements of sodium since more pumps would be required for safety in accident conditions, thereby increasing the plants initial capital costs. However, the normal operations of the reactor would still benefit from the lower pumping power costs in overall electrical production to the grid. Another disadvantage of a sodium cooled ADS design is the possible interaction of a sodium coolant with water used as the working fluid in the power cycle. The reaction between sodium and water is explosive and produces hydrogen a combustible gas.[22] However, reactors utilizing sodium as a coolant and water as the power cycle working fluid have been operated previously in the United States without incident. Therefore, there is an experience base that can be utilized when designing the reactor to alleviate the probability of the interaction between sodium and water in the design.

2.6 MEASURES OF TRANSMUTATION EFFECTIVENESS

The main purpose of this study is to measure the effect various loading patterns or using multiple batches or targets will have on an electron ADS's performance. However, the method of measuring the performance of an ADS is not a straightforward exercise.

There are many possible methods for analyzing the transmutation effectiveness of a system.

The data output from MONTEBURNS allows for some straightforward measures of the transmutation effectiveness of the ADS design such as reduction in TRU mass, radioactivity, radiotoxicity, and heat load generation. The data and results of these measures will be reported in the results of this study; however, analyzing these sets of data individually does not truly represent the effectives of a transmutation system. None of the above values take into account the radiotoxicity or heat load generated by the fission products of the transmuted TRUs. A system that takes into account fission product production and combines these data points together to accurately summarize the system's effectiveness is needed.

Yodersmith developed a new parameter known as the Transmutation System Effectiveness Parameter (TSEP) in an attempt to combine the data regarding radioactivity and heat load as well as accounting for fission product production. TSEP is defined below and takes in data regarding the change in radioactivity and heat load of the TRUs during a transmutation cycle and the radioactivity and heat load of the fission products produced. A TSEP closer to one represents a more effective transmutation system.[10]

$$TSEP = \frac{A_i + H_i}{2(1+P)} \text{ where } P = A_{EOC} + H_{EOC}$$

where A_i is the percent reduction in radioactivity in the TRUs, H_i is the percent reduction in the heat load of the TRUs, A_{EOC} is the percent of the radioactivity at the end of cycle contributed to fission products, and H_{EOC} is the percent of the final heat load

contributed to fission products. The TSEP for each cycle analyzed in this study will be calculated as a method for comparing the various possibilities for the electron ADS design.

3 CONCEPTUAL ADS DESIGN

3.1 TARGET DESIGN

Previous studies as reviewed in the previous sections, utilized either tungsten or uranium for the target material used in the ADS design. When determining whether the use of uranium as the target material is appropriate within a transmutation facility design, the goal of the system must be analyzed. The shear mass of TRUs and FPs currently awaiting disposal indicates that multiple transmutation facilities will be required. Therefore, the facility must be as economically viable as possible to increase the probability of sufficient transmutation capabilities being available without having a negative impact on the economics of nuclear power generation. When attempting to maximize the economic viability and, therefore, efficiency of the system the use of uranium as the target material was considered necessary to reduce the required accelerated electron beam current required for the transmutation facility operation. It is postulated in this study that the increased energy efficiency of the transmutation facility by using uranium offsets the small mass of TRUs that may be produced within the target during exposure to the electron flux.

Utilizing a uranium target in the ADS design, allows for the data presented above for target sizes to be directly applied to this study's design. Therefore, to keep the target small, a 4 cm diameter target was used in the calculations instead of a larger target that would require more modifications of the reactor core for implementation. An ADS system has three main components, the accelerator, neutron producing target, and subcritical core. The design utilized in this thesis assume the target utilized is a cylindrical uranium target 10cm thick with a 4cm diameter.

3.2 ACCELERATOR BEAM

The electron accelerator beam energy used for this study was chosen to be 1,000MeV to take advantage of the higher neutron conversion efficiency within the target material. Although, the total accelerator power required to produce a given number of neutrons is equal in the range of 300-1,000MeV, many accelerators have limited beam current capacities that are more likely to be reached when utilizing a low energy electron beam. For this thesis, a 1,000MeV electron accelerator was used and the beam current was adjusted to achieve the desired k_{eff} within the subcritical core during operation. Beam splitting is utilized in the multiple target analysis portion of this study.

3.3 NEUTRON SPECTRUM

The neutron production within an ADS is limited by the accelerator; therefore, the most efficient use of neutrons is a high priority. This study utilizes a fast spectrum reactor design for the most efficient use of the neutrons produced by the target. The higher fission to capture cross-section ratio for a fast flux of neutrons in the reactor core for TRUs is the motivation behind this decision. The ingestion toxicity levels of the fission products in Figure 2 is much lower than the levels for the TRUs.

3.4 FUEL MATERIALS

The fabrication benefits of metal alloy fuel, along with the established experience base with fertile metal alloy fuel forms, indicate using a metal alloy fuel is the best choice. The choice of a metal alloy fuel over the dispersion fuel is a result of the helium effects reducing the burnup limit advantage of the dispersion fuels. Therefore, the ADS

design studied in this paper utilizes a metal alloy TRU-Zr fuel wrapped in Zr cladding with a maximum of 25w/o TRU in the TRU-Zr.

3.5 CORE COOLANT

When considering the coolant choice for the design of an electron ADS, a primary driving factor is the reduction of uncertainties in a first of its kind design. Therefore, the uncertainties in corrosion problems associated with LBE and lead are weighted heavily when weighing them as options. The use of helium as a reactor coolant in the ADS design is also considered to be adding new levels of uncertainty to the design that may be unnecessary. Sodium as a fast reactor coolant has a large experience base within the United States when compared with the other available options. Therefore, the electron ADS design considered in this study will utilize sodium as the coolant choice.

3.6 MODIFIED ALMR CORE DESIGN

The scope of this study does not allow for the development of a new reactor design for use within the electron ADS; therefore, a previous design was altered for use within the ADS design structure. As mentioned above, a fast reactor utilizing sodium as a coolant is needed for the reactor side of the ADS. A modification of the Advanced Liquid Metal Reactor (ALMR) design developed by GE was chosen for use in the ADS design. The ALMR is a sodium cooled fast reactor design developed by GE using experience gained during the Integral Fast Reactor Program in the United States.

Using a previously designed reactor allows for the assumption that the thermal hydraulics and safety characteristics of the reactor portion of the ADS design are very near to acceptable without the need for an in depth analysis as part of this study.

However, the reactor design does need to be modified slightly to allow for the incoming electron beam and target positioning within the core. As a result, there is no guarantee the safety and thermal abilities of the original design remain intact and a further study would be required to ensure this before moving forward with the proposed reactor design. Therefore, as few changes as possible were made to the ALMR design to allow for its use within the ADS. The primary modification required in the ALMR for use within an ADS is the addition of the target material to the reactor core. The ADS design assumes the target is positioned centrally within the reactor core for all analyses except the multiple target study. In the ALMR design, a control rod is located in the center of the core. Since the ability to cease the production of neutrons within the target via accelerator shut down is considered a safety feature, the removal of the center control element and placement of the target in the resulting space is assumed to be acceptable for this study. With the addition of the target located centrally in the core vertically and horizontally and a beam tube extending from the top of the core to the target, the ALMR design was utilized for all single target results in this study. Figure 20 shows the center fuel assembly with the target located in the interior.

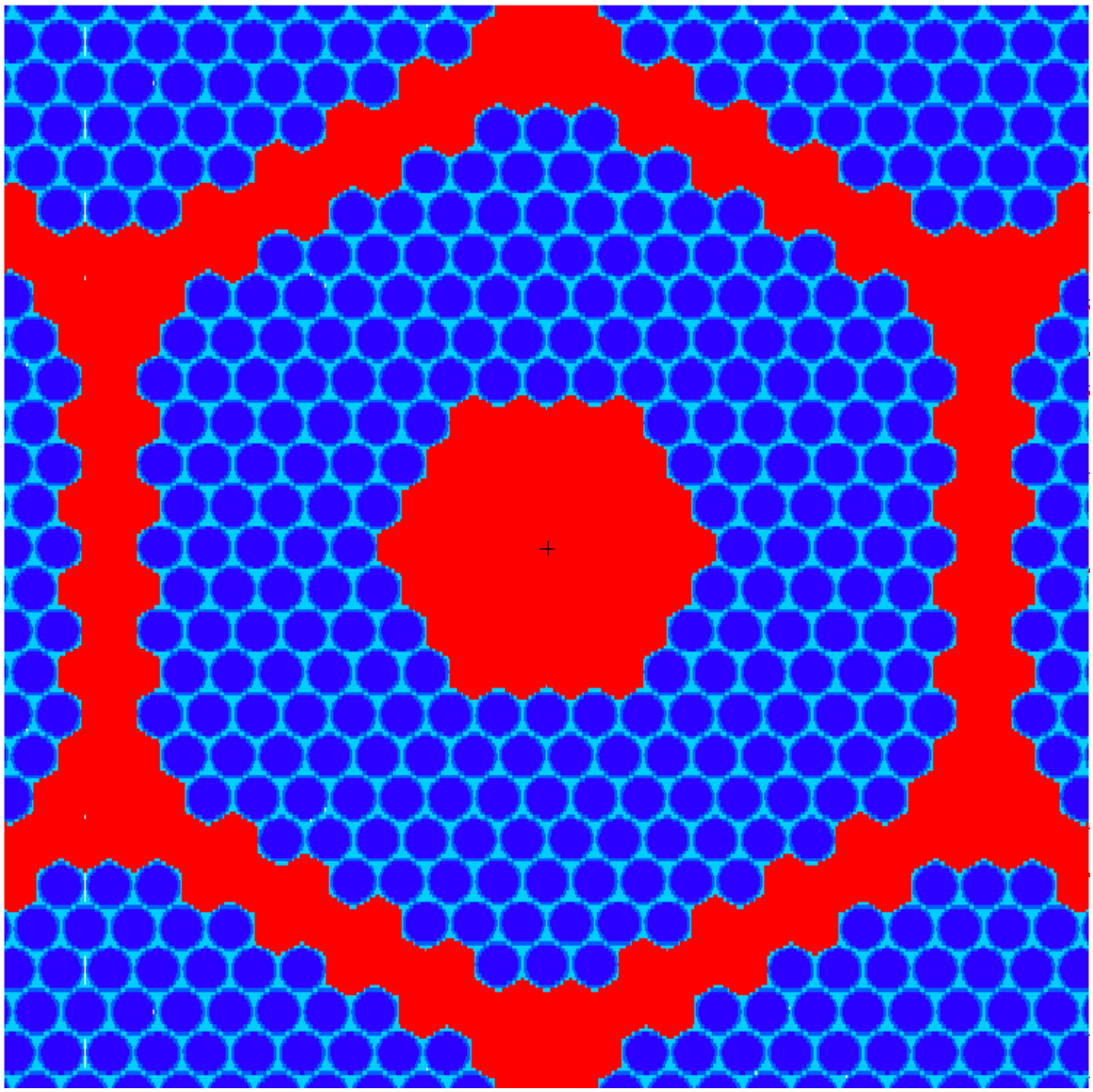

Figure 20: Center Assembly with Target Location

The ALMR design utilizes a triangular fuel rod pitch. The rods are grouped into hexagonal assemblies, 121 of which constitute the entire reactor core. Similar to other fast reactor designs, the fuel rods are placed closely together within an assembly. The rods in an assembly are held together and spaced with a wire wrapper spirally in between the fuel rods. The dimensional characteristics, based on the ALMR design, as utilized in

this study are given in Table 10. A TRU-Zr alloy with Zr cladding was chosen for the fuel form to be used in the ADS design.

Table 10: Reactor Design Characteristics

Characteristic	Value
Core Fuel Height	107cm
Outside Core Barrel Height	147.4cm
Outside Core Barrel Radius	121.10cm
Fuel Radius	0.372cm
Outer Cladding Radius	0.428cm
Fuel Rod Pitch	0.890568cm
Fuel Assembly Pitch	16.14cm

3.7 FAST REACTOR FUEL ISOTOPICS

The fuel utilized in the ADS design is a TRU-Zr alloy mixture clad in Zr. For the loading pattern analysis in this study the fuel alloy was composed of 11w/o TRU within 89w/o Zr. The composition of the TRU portion of the fuel can be tailored by altering the percent of each TRU isotope within the fuel. One of the main goals of this study was to examine the effects of loading patterns to maximize the transmutation efficiencies of the TRUs within the fuel. When determining the composition that would result in a relative burnup rate for each isotope closest to its relative production rate in an LWR many factors would need to be considered. These include the production and destruction of the isotopes within the ADS via means other than fission. Some isotopes are created by the capture of neutrons or beta decays from other isotopes present within the TRU mixture. Therefore, the idea of accurately calculating an exact equilibrium concentration would be a large undertaking and the values would change greatly depending on the loading pattern

utilized. Therefore, the TRU isotopic composition utilized in this study was taken from another equilibrium calculation performed by Bowman for a fast flux reactor.[23] The resulting relative percentages of each TRU isotope in the fuel are shown in Table 11.

Table 11: Overall TRU Fuel Isotopics and for Np-Pu-Am-Cm Fuel Assemblies

TRU Isotope	Percent of Total TRU Composition in Specified Assembly Type Contributed by Isotope
^{237}Np	3.090923
^{238}Pu	6.365206
^{239}Pu	23.23431
^{240}Pu	36.35764
^{241}Pu	6.731925
^{242}Pu	10.73965
^{241}Am	6.155652
^{242}Am	0.785828
^{243}Am	3.221894
^{244}Cm	2.619426
^{245}Cm	0.523885
^{246}Cm	0.159785
^{247}Cm	0.013883

The numbers given in Table 11 are used for calculations performed with all of the TRUs present in a fuel assembly. However, for this study assemblies of the following mixtures of elements were analyzed: Np-Pu-Am-Cm, Np-Pu, Am-Cm, Am, and Cm. Therefore the above numbers, once normalized to account for 11w/o of a fuel assembly can be input directly into the calculations. However, for the other assembly types different numbers must be calculated. The relative abundance of each isotope within a given fuel assembly type are given in Table 12-Table 15. The isotopics for each fuel assembly type were set such that the abundance of each isotope present in the assembly

was the in the same proportion to the other isotopes present in the fuel assembly as they were in Table 11.

Table 12: TRU Isotopics in Np-Pu Fuel Assemblies

TRU Isotope	Percent of Total TRU Composition in Specified Assembly Type Contributed by Isotope
^{237}Np	3.57251
^{238}Pu	7.356948
^{239}Pu	26.85437
^{240}Pu	42.0224
^{241}Pu	7.780805
^{242}Pu	12.41296

Table 13: TRU Isotopics in Am-Cm Fuel Assemblies

TRU Isotope	Percent of Total TRU Composition in Specified Assembly Type Contributed by Isotope
^{241}Am	45.66388
^{242}Am	5.829431
^{243}Am	23.90067
^{244}Cm	19.43144
^{245}Cm	3.886287
^{246}Cm	1.185318
^{247}Cm	0.102987

Table 14: TRU Isotopics in Am Fuel Assemblies

TRU Isotope	Percent of Total TRU Composition in Specified Assembly Type Contributed by Isotope
^{241}Am	60.56701
^{242}Am	7.731959
^{243}Am	31.70103

Table 15: TRU Isotopics in Cm Fuel Assemblies

TRU Isotope	Percent of Total TRU Composition in Specified Assembly Type Contributed by Isotope
^{244}Cm	78.97023
^{245}Cm	15.79405
^{246}Cm	4.817184
^{247}Cm	0.418542

Table 11-Table 15 show the weight percent of the TRU loading that each isotope composes for the various fuel assemblies studied; however, the weight percent of TRU in the fuel was always kept constant at 11w/o in the loading pattern analyses. The overall TRU isotopics listed in Table 11 were also used to determine the number of fuel assemblies of each type to use in the loading patterns discussed below. Excluding the center assembly, which contains the target and Pu, there are 120 assemblies in the core design. If all fuel assemblies contain all for TRUs as listed in Table 11 then all 120 fuel assemblies are the same. However, if the fuel assemblies described in Table 12 and Table 13 are used then by Table 11 a total of 18 of the fuel assemblies need to be Am-Cm while the other 102 are Np-Pu. A third option uses separate fuel assemblies for Am and Cm and utilizes the isotopic abundances listed in Table 12, Table 14, and Table 15. In loading patterns using these fuel assemblies, 6 fuel assemblies use Cm, 12 use Am, and the remaining 102 are Np-Pu. With these options for fuel assembly types, there are nine possible loading pattern types analyzed in the loading pattern analysis portion of this study.

3.8 Loading Patterns for Fast Reactor Analysis

The major analysis performed in this study was to determine the effect using different positions for the various TRU elements within the core. When taking into consideration separations technologies, the four elements, Np, Pu, Am, and Cm, were distributed in the core via multiple loading patterns. When considering proliferation concerns and current separations technologies, Np and Pu were never separated in a loading pattern. Therefore, there are five ways to make fuel assemblies resulting in nine different loading patterns. The first fuel assembly type contains all four TRUs (Np-Pu-Am-Cm) and the core can be loaded with this fuel assembly, all positions containing the same fuel assembly. The core loading pattern using assemblies containing all four TRUs is loading pattern #1 (LP1) and Figure 21 shows the layout of the core where the blue fuel assemblies contain all four TRUs.

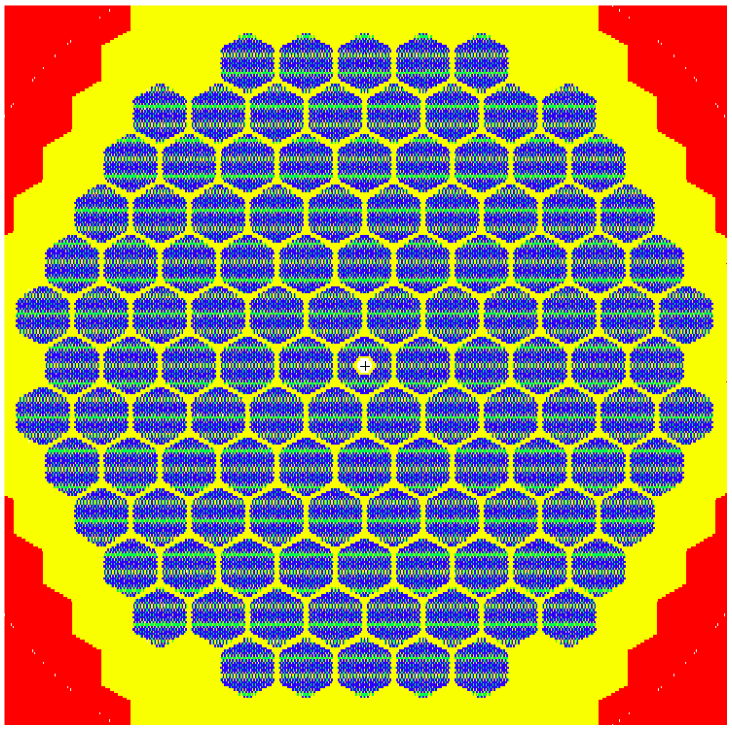

Figure 21: LP1 Core Layout; Blue:Np-Pu-Am-Cm

The next two assemblies types used for the loading pattern analysis contain two TRUs each. The first of these fuel assemblies contains Np-Pu and the second contains Am-Cm. With two different fuel assembly types available for core loading, there are two permutations available. The first permutation shown in Figure 22 is LP2 and uses the Np-Pu assemblies on the inside of the core and the Am-Cm assemblies around the outside edges. The second permutation shown in Figure 23 is LP3 and uses the Am-Cm assemblies in the middle of the core with the Np-Pu assemblies on the periphery.

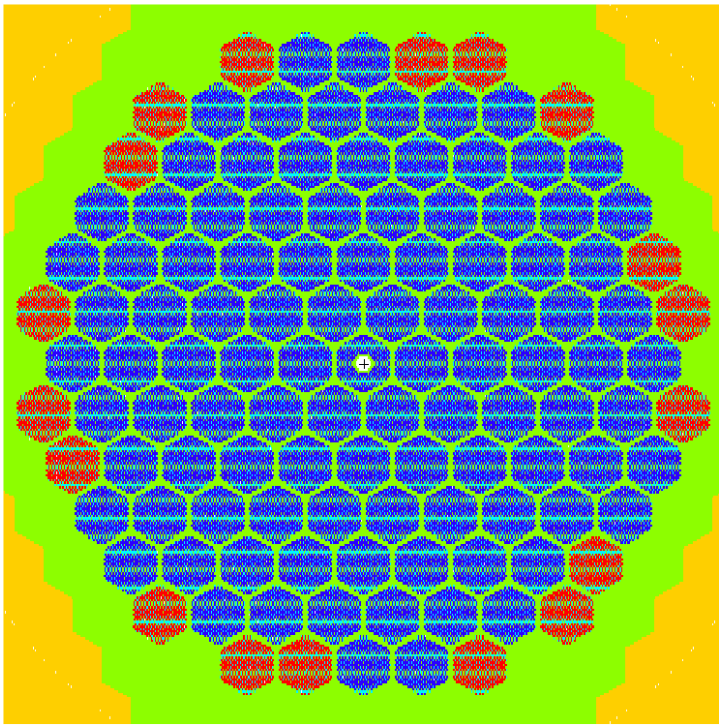

Figure 22: LP2 Core Layout; Blue:Np-Pu, Red:Am-Cm

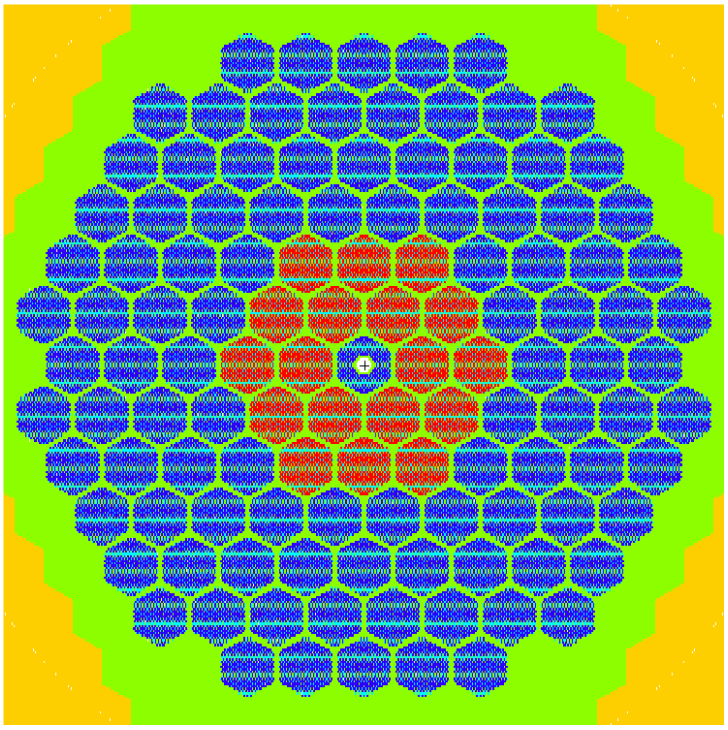

Figure 23: LP3 Core Layout; Blue:Np-Pu, Red:Am-Cm

The last six loading patterns used in the loading pattern analysis utilized three fuel assembly types. The fuel assemblies contained either Np-Pu, Am, or Cm. LP4 shown in Figure 24 used Np-Pu on the inner most assemblies, Am on the middle assemblies and Cm on the outermost assemblies in the core. LP5 on the other hand switched the Am and Cm assemblies such that Np-Pu was still located in the innermost assemblies, Cm assemblies were in the middle ring and Am constituted the outside assemblies as shown in Figure 25. Figure 26 shows LP6, which has Am on the inside, Np-Pu in the middle and Cm on the outside of its core layout. In LP7, Am remained in the inside assemblies, Cm assemblies are now located in the middle region and the Np-Pu assemblies are located externally as shown in Figure 27. Figure 28 depicts LP8 with Cm on the inside, Np-Pu in the middle and Am in the outermost assemblies. Figure 29 showing LP9

maintains Cm on the inside but has Am in the middle assemblies and Np-Pu on the outside. Table 16 summarizes the loading pattern layouts used in this analysis.

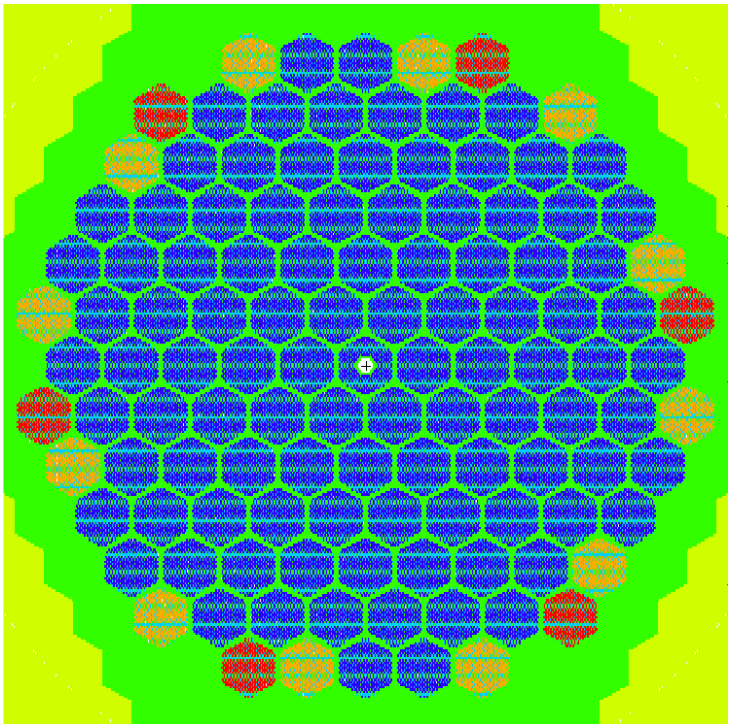

Figure 24: LP4 Core Layout; Blue:Np-Pu, Red:Cm, Orange:Am

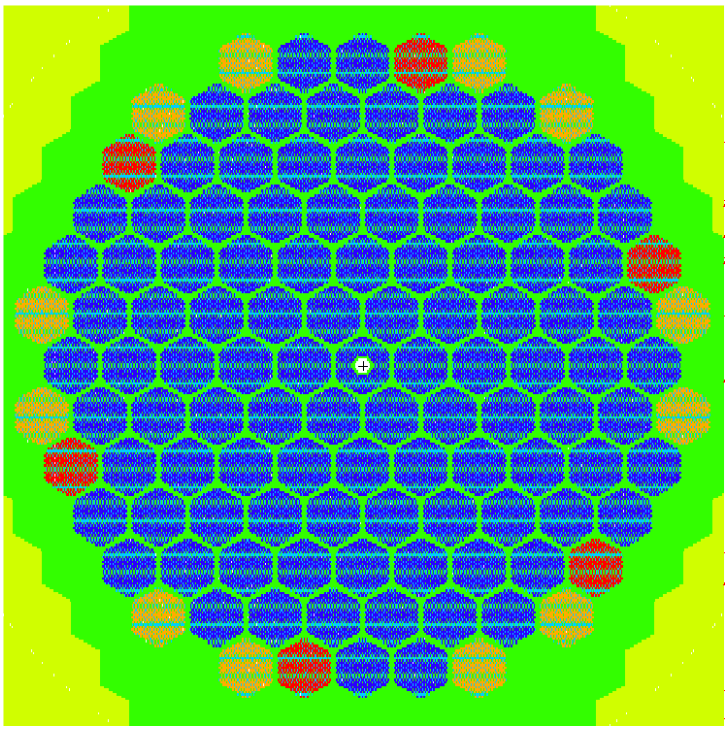

Figure 25: LP5 Core Layout; Blue:Np-Pu, Red:Cm, Orange:Am

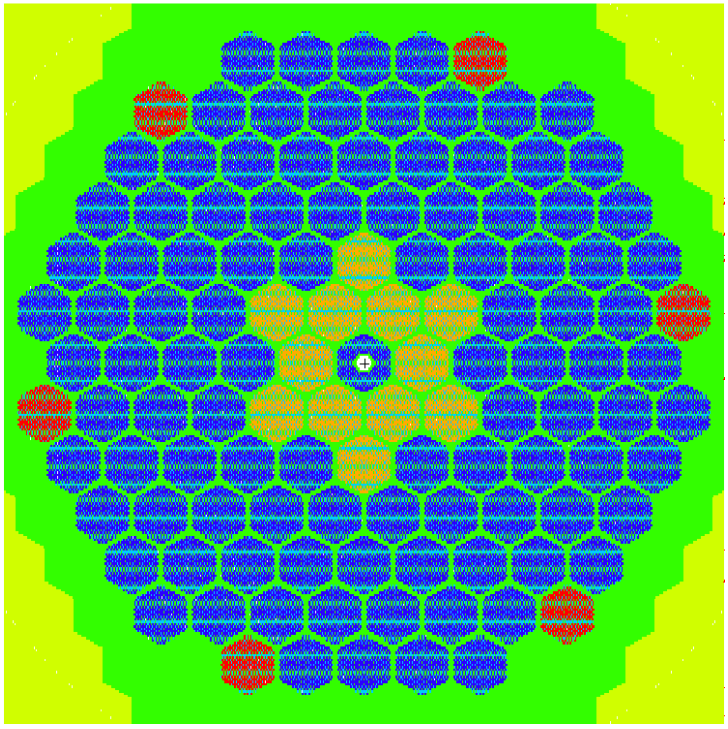

Figure 26: LP6 Core Layout; Blue:Np-Pu, Red:Cm, Orange:Am

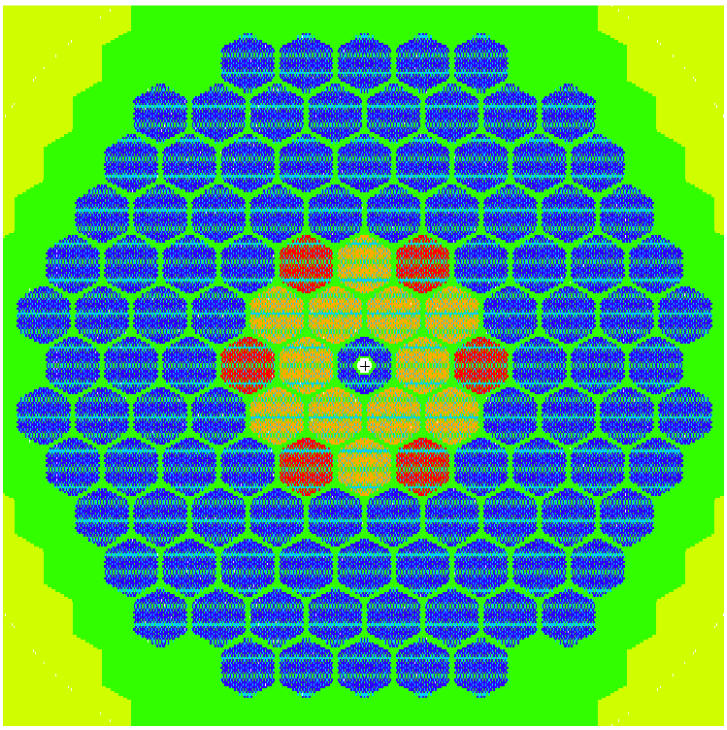

Figure 27: LP7 Core Layout; Blue:Np-Pu, Red:Cm, Orange:Am

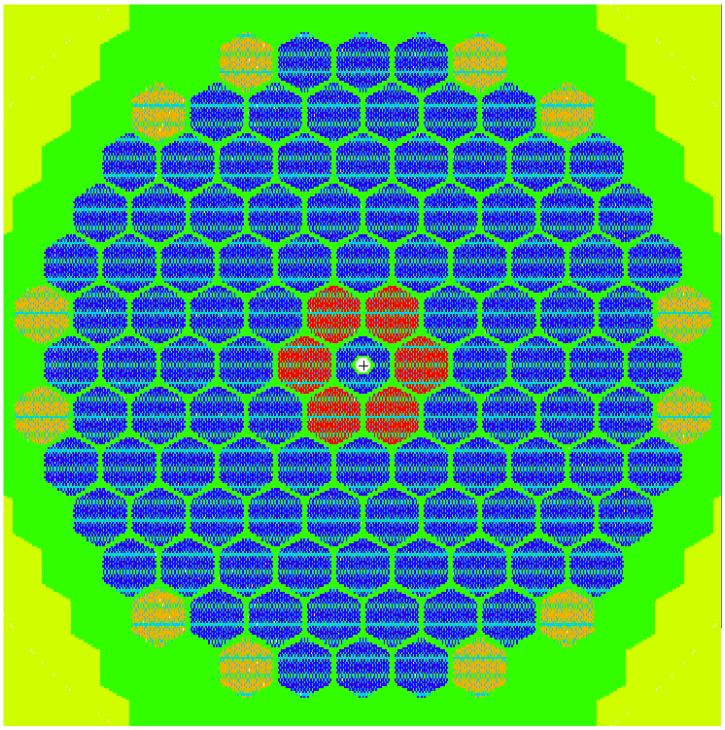

Figure 28: LP8 Core Layout; Blue:Np-Pu, Red:Cm, Orange:Am

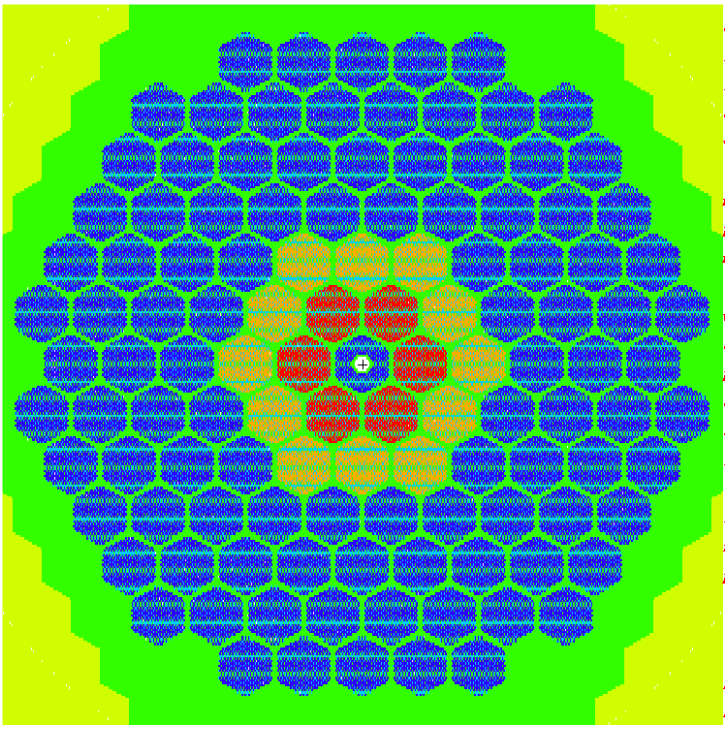

Figure 29: LP9 Core Layout; Blue:Np-Pu, Red:Cm, Orange:Am

Table 16: Loading Pattern Summary

Loading Pattern	TRUs present in Region Listed		
	Inner Region	Middle Region	Outer Region
1	Np-Pu-Am-Cm		
2	Np-Pu		Am-Cm
3	Am-Cm	Np-Pu	
4	Np-Pu	Am	Cm
5	Np-Pu	Cm	Am
6	Am	Np-Pu	Cm
7	Am	Cm	Np-Pu
8	Cm	Np-Pu	Am
9	Cm	Am	Np-Pu

3.9 MULTIPLE BATCH CORE DESIGN STUDY

The major focus of this paper has been an analysis of various loading patterns that could be utilized within the electron ADS design put forth within this project. In the loading pattern analysis, it was assumed that the whole reactor core in the ADS design would be reloaded during each shutdown. However, power reactors typically replace only around one third of the fuel each cycle. It is possible that employing a similar methodology for the ADS would be beneficial. Therefore, a small study was performed using a three batch principle for the core loading in the ADS design.

The analysis performed to determine the correct isotopics for each batch in the reactor core used a simplified approach. First, the core was analyzed for 18 months with all fresh fuel assemblies containing Np-Pu-Am-Cm with the isotopics listed in Table 11. The isotopics of the fuel after this run was then considered to be the composition of the once burnt fuel for the remainder of this study. Then an analysis with the core completely loaded with once burnt fuel was performed for another 18 month cycle. The resulting composition of the fuel after the second 18 month cycle was considered twice burnt fuel for the rest of the study. The isotopics of the once burnt fuel are listed in Table 17 while the isotopics of the twice burnt fuel are listed in Table 18.

Table 17: Isotopics of Once Burnt Fuel

TRU Isotope	Percent of Total TRU Composition in Once Burnt Fuel from Isotope
^{237}Np	2.49
^{238}Pu	7.00
^{239}Pu	17.62
^{240}Pu	38.87
^{241}Pu	7.83

Table 17 Continued

^{242}Pu	12.28
^{241}Am	5.15
^{242}Am	0.46
^{243}Am	3.80
^{244}Cm	3.48
^{245}Cm	0.76
^{246}Cm	0.23
^{247}Cm	0.02

Table 18: Isotopics of Twice Burnt Fuel

TRU Isotope	Percent of Total TRU Composition in Twice Burnt Fuel from Isotope
^{237}Np	1.98
^{238}Pu	7.15
^{239}Pu	13.43
^{240}Pu	40.28
^{241}Pu	8.59
^{242}Pu	13.80
^{241}Am	4.36
^{242}Am	0.33
^{243}Am	4.32
^{244}Cm	4.39
^{245}Cm	1.03
^{246}Cm	0.32
^{247}Cm	0.03

In the multiple batch study, the overall reactivity of the TRUs in the fuel for a loading is reduced due to burnup of the fuels at the beginning of the cycle. To compensate for this, the TRUs constituted 15w/o of TRU-Zr alloy mixture in the fresh

fuel rods, which is higher than the 11w/o used in the loading pattern analysis. The loading pattern used for the multiple batch core is shown in Figure 30.

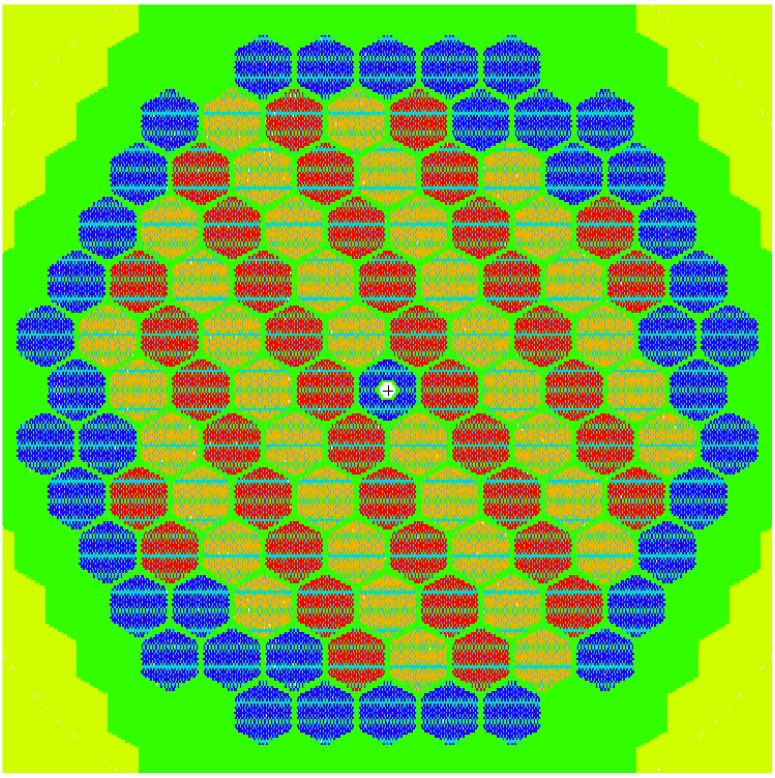

Figure 30: Multiple Batch Core Layout; Blue-Fresh Fuel, Red-Once Burnt, Orange-Twice Burnt

3.10 MULTIPLE TARGET DESIGN STUDY

In an ADS design, one of the primary concerns within the reactor core is higher peaking factors due to the large flux of neutrons emitted from the target. In the loading pattern and multiple batch studies presented in this paper, the target is located in the center of the core further increasing the possibility of high peaking factors in the reactor. One possible method of alleviating the high peaking factors is to move the target away from the center of the core. However, in order to maintain core symmetry, this would require multiple targets. With an electron ADS the use of multiple targets is a possibility due to the small overall size of the targets when compared to the size of the core.

Therefore, an analysis was performed using three targets within the core to determine the effect on peaking factors. The core layout is shown in Figure 31. The isotopics of the TRU in the fuel for this core were the same as those given in Table 11; however, the TRUs only accounted for 9.87w/o in the TRU-Zr alloy in the fuel to maintain a suitable k_{eff} level within the core during the cycle. The 9.87w/o was utilized because after initially running MONTEBURNS with 11w/o it was realized this would result in a k_{eff} much higher than all of the other loading patterns. Therefore, after some trial and error runs to determine a w/o that would result k_{eff} values on par with the other loading patterns, 9.87w/o was chosen.

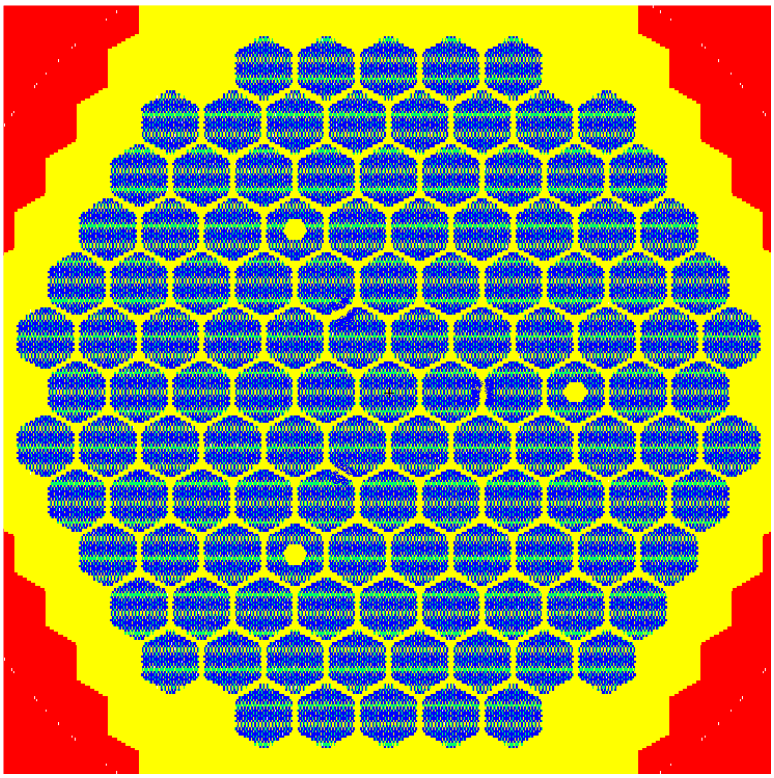

Figure 31: Multiple Target Core Layout

3.11 INGESTION RADIOTOXICITY AND HEAT LOAD REDUCTION PARAMETER

However, another parameter, which utilizes radiotoxicity as a replacement for radioactivity within the TSEP, will also be utilized. Utilizing radiotoxicity instead of radioactivity will help when analyzing the various loading patterns, which may result in preferential burnup of certain TRUs with more radiotoxic decay patterns. As discussed above, the primary pathway for human exposure to waste in Yucca Mountain is via ingestion of contaminated groundwater; therefore, the new parameter will utilize the ingestion radiotoxicity data provided by MONTEBURNS.

The new parameter for use as a measure of the ADS design's transmutation effectiveness is the Ingestion Radiotoxicity and Heat load Reduction Parameter (IRHRP). This new parameter will use data for the ingestion radiotoxicity and heat load of the TRUs initially loaded into the core for comparison with the production of heat loads due to fission product buildup within the fuel. The structure of the IRHRP is very similar to the TSEP and only attempts to more properly account for the preferential burnup of certain TRUs within a loading pattern, which is represented by the ingestion radiotoxicity of the TRUs in the fuel after a cycle. Also, since the radiotoxicity of the fission products produced is dominated at EOC by fission products that will be decayed away before the expected failure time of the Yucca Mountain waste packages, the End of Cycle radiotoxicity from fission products is not accounted for. Some fission products do contribute greatly to the long term dose from Yucca Mountain (^{99}Tc and ^{129}I) because of their water solubility. However, from Figure 2, the ingestion radiotoxicity the radiotoxicity of fission products at EOC is dominated by ^{90}Sr and ^{137}Cs which are

expected to decay significantly by ~1,000yrs versus a waste package lifetime expected to be 10,000yrs. The formula for IRHRP is given below.

$$IRHRP = \frac{R_i + H_i}{1 + H_{EOC}}$$

Where R_i is the percent reduction in ingestion radiotoxicity in the TRUs, H_i is the percent reduction in the heat load of the TRUs, and H_{EOC} is the percent of the final heat load contributed to fission products.

4 METHODOLOGY

4.1 CODES UTILIZED

The analyses performed for this study utilized three codes heavily. The three codes used to do the majority of the calculations are MCNPX, Orgien2, and MONTEBURNS. The abilities and limitation of these codes as they pertain to this study are discussed below.

MCNPX is a Monte Carlo based transport code built as an extension upon MCNP to cover more energies and particles. In this study, MCNPX takes the ADS reactor core design, including geometry and materials, and given a source term within the target material can track a source neutron and the particles it produces. As MCNPX tracks more and more source neutrons a general map of the behavior of the core can be developed. MCNPX uses an extensive cross section data library based primarily on ENDF files when calculating the behavior of a particle. MCNPX is used for this study instead of MCNP due to its support of higher energy neutrons, which are emitted from the target during ADS operations. The user can setup tallies within the MCNPX run in order to gather data on the neutron flux distribution within the core. This study utilized these tallies to gain an approximation of the peaking effects within the core. The flux distribution within the core was also used to determine transmutation rates of the TRUs of interest in the ADS design.[24]

Origen2 is a computer code that calculates the buildup, decay, and processing of radioactive materials. Given a neutron flux, Origen2 can calculate the changes experienced by materials, such as the TRUs in the ADS fuel, due to burnup and decay

chains. Origen2 uses an extensive data library of cross sections to calculate the changes in mass of the materials studied in a problem.[25]

MONTEBURNS can calculate coupled neutronics/isotopics problems for nuclear systems. MONTEBURNS is an automated method of coupling MCNP or MCNPX with Origen2 or other burnup/depletion codes. By linking these two codes, MONTEBURNS allows for an analysis of the rate of transmutation within the ADS and a measure of the change in reactivity of the system throughout a cycle. Given an initial geometry and material composition, MONTEBURNS uses MCNPX to calculate the flux distribution with the core. This data is then fed to Origen2, which can calculate the depletion and burnup of the isotopes in the fuel exposed to the neutron flux. Origen2 can then determine the new isotopic compositions of the fuel after a given time step. The new isotopics can be fed back into MCNPX by MONTEBURNS to allow for the calculation of a new flux distribution. This process can be repeated to allow for multiple time steps to be calculated throughout an ADS cycle. MONTEBURNS also uses a simple predictor-corrector method during the cycling process.[26]

Utilizing MONTEBURNS allows for determining both the neutronics behavior of the ADS over a cycle and the efficiency of the ADS in transmutation the TRUs loaded in the fuel. As MONTEBURNS progresses through the calculations for a cycle, the k_{eff} and flux distribution at each time step can be calculated. Therefore, the change in k_{eff} for a cycle will be known. Calculating the change in k_{eff} over a cycle is important for an ADS because the accelerator beam current will have to be increased or decreased to keep the system at criticality as the reactivity of the fuel changes. It is beneficial to keep the amount of current changes required from the accelerator beam as small as possible to

maximize the investment made in the capital cost of the accelerator by using it to its full potential at all times. Therefore, the k_{eff} results provided by MONTEBURNS at each time step are an important tool in analyzing an ADS design. MONTEBURNS, along with tallies from within MCNPX, can be used to determine the peaking factors within a reactor at each time step as well. With this information, an analysis can more accurately determine the maximum peaking factor obtained during a cycle by a particular core design or loading pattern. MONTEBURNS also provides data on the material isotopics, radiotoxicity, and heat load at each time step. This data is important in evaluating the transmutation effectiveness of the ADS design and loading pattern. Therefore, the data MONTEBURNS provides at each time step can be used to compare various loading patterns to determine which has the best neutronics behavior and transmutation effectiveness.

4.2 BENCHMARK

This study analyzes an ADS system using a 1GeV electron accelerator and a fast reactor based on the ALMR design. There is no experimental data available for direct benchmarking of the results derived in this study. However, as a check on the accuracy of the input files developed for MCNPX and MONTEBURNS, code runs similar to ones performed previously by Yodersmith[10] can be analyzed to compare the resulting output. The analyses performed by Yodersmith were very similar to those performed in this study.[10] The only geometry differences in the two studies were the size of the target and the addition of a beam tube in this study's setup. There are also differences in the fuel loading between the two studies. However, to modify an input file from one study to work for the other study is a simple process. Therefore, modifying the input files from

this study to match the geometry and material compositions present in the previous study was seen as a benchmarking of the input file accuracy.

Three loading patterns analyzed by Yodersmith were modeled with modified input files from this study to determine if there were any discrepancies. The structure of the input files was different; however, the geometry, materials, and other aspects of the problem analyzed were identical between the input files with the exception of the inclusion of a beam tube in the new input files. The results from the new input files are compared with the previous study's results in Table 19-Table 21.[10]

Table 19: Comparison of Reference 10's LP1 k_{eff} Results with New Input File's Results

Time Step	Reference 10 k_{eff} Result	New Input File k_{eff} Result	Percent Difference
1	0.93781	0.93701	0.085305
2	0.90166	0.90223	0.063217
3	0.83016	0.82358	0.792618
4	0.7434	0.7459	0.336293
5	0.65856	0.64985	1.322583
6	0.59396	0.60002	1.020271
7	0.55432	0.55939	0.914634
8	0.55432	0.55939	0.914634
9	0.55432	0.55939	0.914634

Table 20: Comparison of Reference 10's LP9 k_{eff} Results with New Input File's Results

Time Step	Reference 10 k_{eff} Result	New Input File k_{eff} Result	Percent Difference
1	0.79626	0.77343	2.867154
2	0.82958	0.82294	0.800405
3	0.88122	0.89255	1.285718
4	0.91602	0.92173	0.623349
5	0.93823	0.93726	0.103386

Table 20 Continued

6	0.9562	0.95115	0.528132
7	0.96637	0.96365	0.281466
8	0.96637	0.96365	0.281466
9	0.96637	0.96365	0.281466

Table 21: Comparison of Reference 10's LP19 k_{eff} Results with New Input File's Results

Time Step	Reference 10 k_{eff} Result	New Input File k_{eff} Result	Percent Difference
1	0.88586	0.88936	0.395096
2	0.90038	0.90379	0.378729
3	0.92759	0.92766	0.007546
4	0.93246	0.93347	0.108316
5	0.94089	0.93948	0.149858
6	0.95014	0.94669	0.363104
7	0.95053	0.95154	0.106257
8	0.95053	0.95154	0.106257
9	0.95053	0.95154	0.106257

From the data above, we can see that the largest percent difference in the k_{eff} results is 2.867% shown in Table 20. For comparison, the relative uncertainty in the k_{eff} from MCNPX for this result was 1.043%. Therefore, it can be assumed that the discrepancies in the k_{eff}'s calculated with the old and new input files is a function of the uncertainties within MCNPX and not an error in the file setup.

4.3 ANALYSES PERFORMED

When performing the analyses presented in this study, the power of the reactor in the electron ADS design was always assumed to be operating at 500MW during the entire cycle. For all computer runs performed, MONTEBURNS performed five Origen2

calculations per time step and the time steps analyzed were always six months in length. During the calculations for the loading pattern analysis and multiple target analysis, the core was operated for a twenty four month cycle. However, for the multiple batch analysis the cycle length was reduced to eighteen months.

5 RESULTS

5.1 NEUTRONICS RESULTS AND DISCUSSION FROM LOADING PATTERN ANALYSIS

The important factors when investigating the neutronics behavior of the various possible loading patterns in an electron ADS are the changes in k_{eff} during the cycle and the peaking factors observed within the reactor core. The changes in k_{eff} during a cycle are important once the role of the accelerator in the ADS is understood. Some reactivity control via control elements may be necessary within an ADS core; however, it is very likely that some reactivity control will be performed by changing the accelerator beam current used during operations. If the electron accelerator beam current is reduced, less neutrons will be produced in the target within the core which will reduce the reactivity of the core and likewise an increase in accelerator beam current will increase the reactivity of the core by supplying a larger source of neutrons from the target. Changing the accelerator beam current should be kept to a minimum in order to maximize the capital cost investment placed in the construction and operation of the accelerator for the ADS. Therefore, loading patterns with low k_{eff} swings during a cycle can more effectively utilize the benefit the accelerator provides in an ADS.

During the loading pattern analysis, the TRU loading within the fuel alloy was kept constant at 11w/o. However, the TRU-Zr alloy can handle up to 25w/o TRU within the matrix. Therefore, since the w/o was kept constant, some loading patterns may have higher overall k_{eff} values, but it should be remembered that the k_{eff} of any loading pattern can be increased by increasing the loading of TRU within the fuel matrix. Therefore, instead of analyzing the k_{eff} values obtained from MONTEBURNS to determine which loading pattern had the lowest or highest value, the change in k_{eff} over the cycle will be

the primary value analyzed. However, the minimum, maximum, and average k_{eff} for each loading pattern over the cycle will also be reported, but more emphasis should be placed on the range the k_{eff} exhibits over the cycle because this is a more accurate measure of the changes in accelerator beam current that may be required. As a reminder, the description of the loading patterns analyzed is given again in Table 22.

Table 22: Loading Pattern Summary

Loading Pattern	TRUs present in Region Listed		
	Inner Region	Middle Region	Outer Region
1	Np-Pu-Am-Cm		
2	Np-Pu		Am-Cm
3	Am-Cm	Np-Pu	
4	Np-Pu	Am	Cm
5	Np-Pu	Cm	Am
6	Am	Np-Pu	Cm
7	Am	Cm	Np-Pu
8	Cm	Np-Pu	Am
9	Cm	Am	Np-Pu

A summary of the k_{eff} characteristics observed for each loading pattern during the cycle is given in Table 23. From the table, the data shows that the loading pattern with the lowest k_{eff} swing during the cycle is LP7. The next two lowest in order are LP9 and LP3. All of these loading patterns have the Np-Pu assemblies located on the periphery of the core. The average k_{eff} for these loading patterns were also the lowest values. This indicates, as might be expected, that the Np-Pu assemblies burnup more quickly, and therefore reduce in reactivity, than the Am or Cm containing assemblies. Therefore, placing the Np-Pu on the periphery allows for a more consistent k_{eff} because they

experience less burnup; however, the TRU loading in the fuel would have to be increased in these loading patterns to make up for the lower overall reactivity. On the other hand, loading patterns with Np-Pu in the center of the core experienced the largest reactivity swings and also exhibited the highest average k_{eff} values. If Np-Pu, is on the outside of the core, the difference between LP7 and LP9 seems to indicate using Am in the innermost assemblies is more beneficial than Cm in terms of k_{eff} swings. However, as observed in LP6 and LP8, if Np-Pu is in the middle location there is not a significant difference between having Am or Cm in the innermost location. A similar observation from LP4 and LP5 exists for having Np-Pu as the innermost assembly type.

Table 23: Loading Pattern k_{eff} Results

LP#	Average K_{eff}	Maximum K_{eff}	Minimum K_{eff}	K_{eff} Range
1	0.913856	0.9561	0.86149	0.09461
2	0.935056	0.97941	0.88332	0.09609
3	0.894504	0.92857	0.85519	0.07338
4	0.938556	0.98546	0.88646	0.099
5	0.940432	0.9866	0.88642	0.10018
6	0.902552	0.94514	0.85682	0.08832
7	0.898168	0.93119	0.866	0.06519
8	0.941166	0.98071	0.89135	0.08936
9	0.909038	0.9408	0.86881	0.07199

The k_{eff} of each loading pattern as a function of the time step is shown in Figure 32. As shown in the figure, the k_{eff} for all of the loading patterns decreases over the entire cycle. Also shown in the figure, the loading patterns with lower k_{eff} swings, such as LP7, show a fairly linear association between burnup time and k_{eff} while some of the

loading patterns with higher k_{eff} swings, such as LP4, show more variability in the shape of the curve.

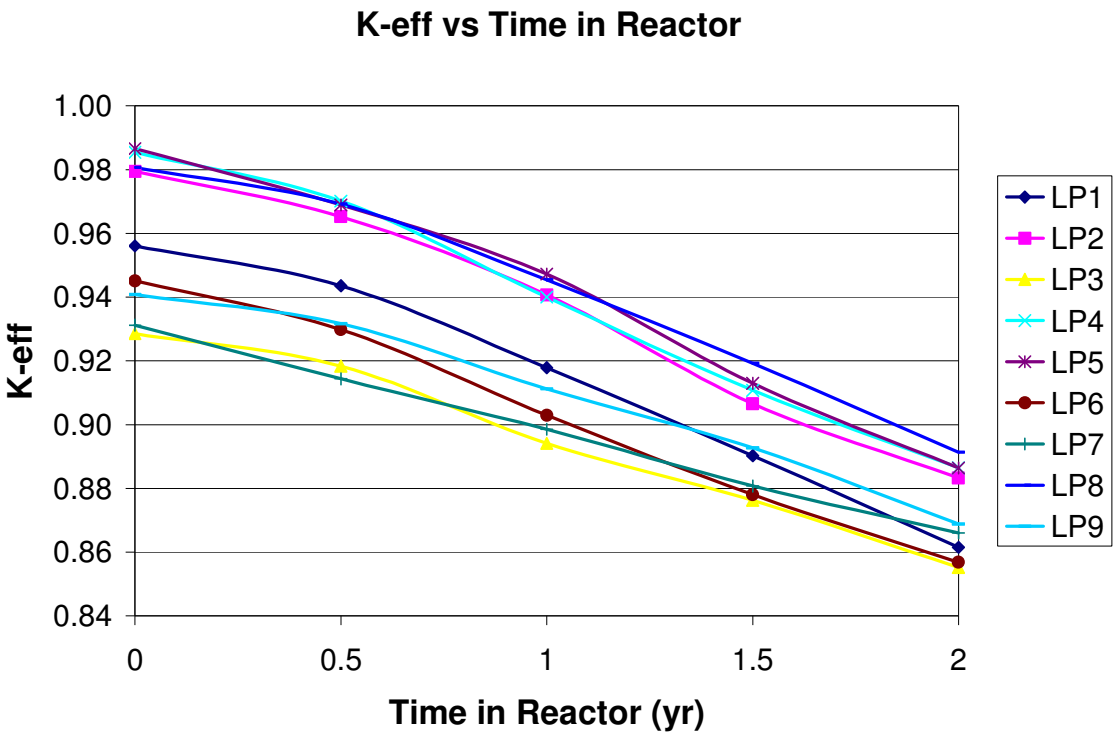

Figure 32: Loading Pattern k_{eff} vs Time

The second major neutronics characteristic analyzed for each loading pattern is the peaking factors observed within the reactor core throughout a cycle. Peaking factors affect the thermal performance of the system. High peaking factors require reducing the overall power output of the core in order to maintain the hottest locations within safety limits. On the other hand, low peaking factors allow the core to run at a higher thermal output while still maintaining all fuel rods within safety limits. In an ADS design, it is beneficial to maximize the thermal output of the core in order to maximize the amount of electrical energy that can be extracted during core operations. Since there is a large volume of TRUs from LWR operations to be transmuted, many ADS facilities would be

required and therefore, making the ADS as economically viable as possible is a necessary goal. Lower peaking factors allow more electrical energy to be produced in a given core, which can then be sold on the electrical grid to recoup the capital and operational costs of the facility.

The peaking factors obtained for each loading pattern are listed in Table 24, along with the maximum linear heat generation rate observed. Table 24 provides information on the lowest peaking observed in the core for a time step, the average peaking observed over all time steps, the maximum peaking observed for a time step, and the maximum linear heat generation rate for the maximum peaking observed during a time step.

Table 24: Loading Pattern Peaking Factor Results

LP#	Average Peaking Factor	Minimum Peaking Factor	Maximum Peaking Factor	Maximum Linear Heat Rate (W/cm)
1	4.9	3.8	6.1	867.2
2	4.2	3.1	5.7	809.4
3	5.8	5.1	7.0	995.3
4	4.6	3.2	6.6	941.2
5	4.1	2.9	5.5	786.9
6	5.6	4.0	6.8	964.1
7	5.8	4.6	7.0	991.6
8	4.4	3.2	5.8	826.1
9	5.9	5.1	6.4	913.2

Table 24 shows the loading patterns that had the most beneficial k_{eff} behavior are also the ones with the worst peaking factors within the core. The peaking factors for an ADS design are always going to be worse than those observed in a typical power reactor due to the large source of neutrons emitted from the target location in the core.

Therefore, some idea of acceptable peaking factors within an ADS is needed. For an sodium cooled ADS based on the ALMR design utilizing a low TRU loading (~10%) within a metallic fuel, the maximum linear power rate for meeting safety limits is 450W/cm[27]. None of the loading patterns analyzed in this study meet this criterion even for a thermal power level of 500MW. The target thermal power level of an ADS based on an ALMR like reactor core is 840MW, which results in even higher linear power rates within the currently designed ADS.[27]

Although none of the loading patterns analyzed exhibited acceptable power peaking levels, it is still important to analyze the characteristics that control power peaking levels among the loading patterns. The lowest peaking factors occurred when the Np-Pu loaded fuel assemblies were located in the center of the core. However, unlike the k_{eff} calculations were the location of the Np-Pu assemblies seemed to be the only driving factor, the placement of the Am and Cm assemblies has an effect on the peaking factors observed. When analyzing LP4 vs LP5, LP6 vs LP8, and LP7 vs LP9, with the Np-Pu assemblies in the same location within a pair, the placement of Cm closer to the center of the core results in lower maximum peaking factors. Figure 33 shows the peaking factor of each loading pattern as a function of time. An interesting thing to note from the figure is that although in general the trend is an increasing peaking factor throughout the cycle, there are some irregularities. For example, LP4 has a dramatic decrease in peaking factor over the last six months of operations. The overall behavior of the peaking factor throughout a cycle should be analyzed further. However, to facilitate comparison of the loading patterns analyzed, the maximum observed peaking factor in a cycle appears to be the most importantfactor.

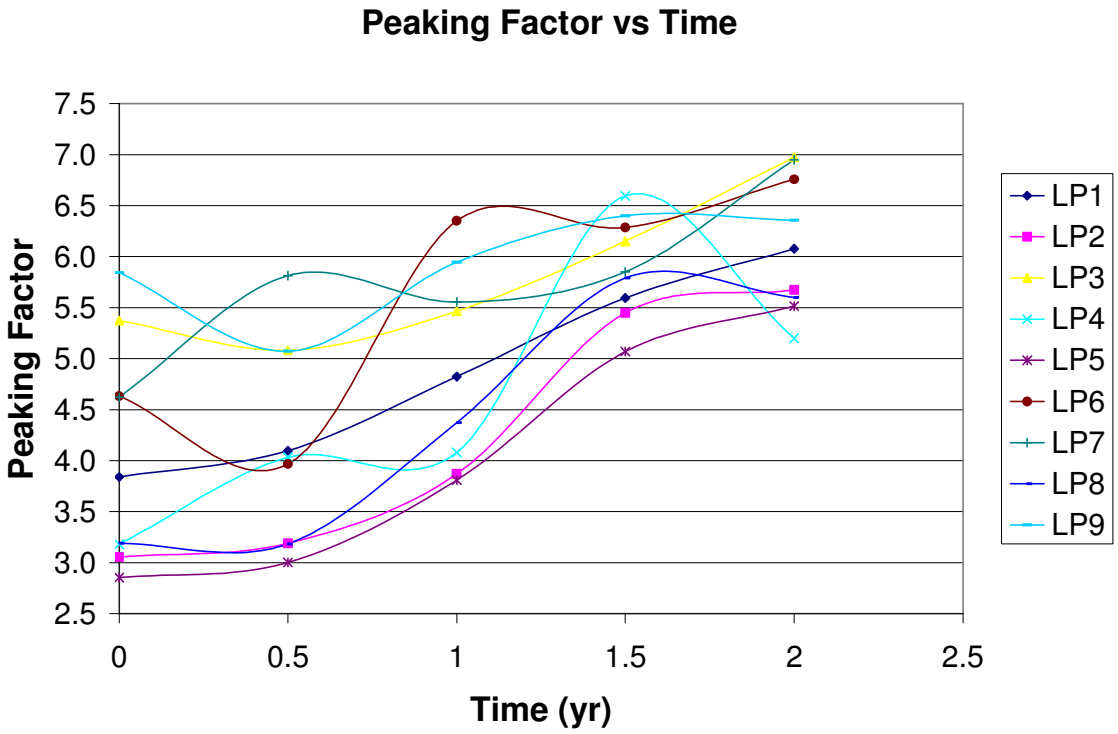

Figure 33: Loading Pattern Peaking Factors vs Time

The neutronics behavior results of the loading patterns analyzed does not clearly distinguish one loading pattern as optimal. The loading patterns with better k_{eff} behaviors typically had worse peaking factors and vice versa. None of the loading patterns exhibited peaking factors that would be acceptable for a final ADS design using a sodium cooled reactor system similar to the ALMR. The k_{eff} swings observed in the loading patterns was also unacceptable from an economics point of view. Various methods can be employed to improve the k_{eff} and peaking factor behavior of the system. Examples of these methods include the use of poisons or reflectors within a core design. Detailed investigations of these methods are however beyond the scope of this study. In this study, the transmutation effectiveness of the loading patterns analyzed was mainly examined to

determine which loading pattern would have the most success within the currently designed ADS.

5.2 Transmutation Results and Discussion from Loading Pattern Analysis

The transmutation effectiveness of a system can be measured with several different methods. This study attempts to investigate several of these methods in determining which loading pattern analyzed was the most efficient at transmuting the TRUs loaded into the core. The various quantities that have been used to describe the effectiveness of a transmutation system, including TRU mass, radioactivity, heat load, and radiotoxicity reduction, will be analyzed first. Parameters such as the TSEP and IRHRP that combine these values will also be calculated and analyzed.

The total TRU mass reduction experienced for all of the loading patterns analyzed was ~20%. Although, there were some variations in the mass of each fuel assembly type transmuted, the overall TRU mass reduction for all the loading patterns can be considered almost identical. The fuel assemblies close to the center of the core experienced higher burnups, and therefore the TRUs present in those fuel assemblies experienced more burnup than the other TRUs in the fuel. Further analysis of the individual TRU mass reductions was not deemed necessary since the preferential burnup of certain TRUs in a loading pattern would show up more effectively in the radioactivity and radiotoxicity analyses.

The toal radioactivity levels in the core are another variable used to measure transmutation effectiveness. Table 25 gives the results for the loading pattern analysis by reporting the percent reduction in actinide radioactivity and percent of EOC radioactivity from fission products for each loading pattern. The reduction in actinide radioactivity

shows LP8 and LP9 as the most effective setups for transmutation. Both of these loading patterns utilize Cm loaded in the innermost fuel assemblies. Another interesting result is that the loading patterns with less separation of the TRUs, such as LPs 1-3, exhibited a lower percent reduction in actinide radioactivity. For all cases the trend is a steady decline in actinide radioactivity throughout the cycle.

Table 25: Loading Pattern Radioactivity Data

LP #	Percent Reduction in Actinide Radioactivity	Percent of EOC Radioactivity from Fission Products
1	1.0	99.2
2	5.2	99.3
3	6.3	99.3
4	13.0	99.3
5	13.1	99.3
6	12.3	99.3
7	15.2	99.3
8	19.1	99.3
9	17.8	99.3

The heat load of LWR waste is important in directly affecting the capacity of Yucca Mountain for power reactor waste. An effective transmutation system should maximize the reduction of the heat load through waste burning in order to maximize the waste disposal capacity provided by Yucca Mountain. Table 26 summarizes the results of the analysis regarding heat load reduction as the percent reduction in actinide heat load and percent of EOC heat load contributed by fission products. The percent heat load at EOC contributed by fission products was not much different among the loading patterns. LP8 and LP9 again show they are most effective in transmuting the TRUs present in the fuel with the greatest percent reduction in actinide heat load and radioactivity from

above. LP7 is also once again the third best separating itself from the rest of the loading patterns but still not close to either LP8 or LP9. LPs 1-3 show low reductions in heat load as well as radioactivity. LP1 actually shows an increase the actinide heat load throughout the cycle.

Table 26: Loading Pattern Heat Load Data

LP #	Percent Reduction in Actinide Heat Load	Percent of EOC Heat Load from Fission Products
1	-4.4	99.1
2	3.9	99.3
3	13.6	99.4
4	27.9	99.4
5	28.4	99.4
6	29.8	99.4
7	39.8	99.5
8	48.9	99.5
9	49.1	99.6

The final value reported by MONTEBURNS analyzed for a measure of the system's transmutation effectiveness is the radiotoxicity. The ingestion and inhalation radiotoxicity are reported from within MONTEBURNS and are a clearer measure of the reduction in risk from the TRUs than the radioactivity. Although the most likely pathway for exposure to waste from Yucca Mountain by the public involves the ingestion radiotoxicity, the inhalation toxicity is also presented in this report. However, only the ingestion radiotoxicity is used in the IRHRP. In Table 27 LP8 and LP9 again demonstrate the most effective transmutation ability for the currently designed ADS. LP7 also once again is the third best separating itself from the rest of the loading patterns but not as good as LP8 and LP9.

Table 27: Loading Pattern Radiotoxicity Data

LP #	Percent Reduction in Inhalation Radiotoxicity	Percent Reduction in Ingestion Radiotoxicity
1	4.8	1.7
2	16.2	10.6
3	18.2	17.7
4	25.0	27.9
5	25.0	28.3
6	24.7	29.4
7	28.6	37.1
8	32.8	44.1
9	32.2	44.1

This study will look at two parameters (i.e., TSEP and IRHRP) which attempt to combine the relevant data from above into one number representing the overall transmutation effectiveness of the ADS design analyzed. The TSEP analyzes the radioactivity and heat load of the TRUs in the fuel and the fission products produced. The IRHRP, on the other hand, uses ingestion radiotoxicity instead of radioactivity in an attempt to recognize the uneven burnup of TRUs during a cycle and the most likely exposure path to Yucca Mountain waste. The IRHRP also does not take into account the radiotoxicity or radioactivity of the produced fission products since the fission product isotopes that would contribute the most to these values will have decayed away by the time any Yucca Mountain waste packages are expected to fail. The TSEP and IRHRP are shown in Table 28. As discussed with the results of other measurements for transmutation effectiveness, LP8 and LP9 are the most effective transmutation loading patterns out of the nine analyzed. LP7 is again the third most effective, as would be expected since both parameters are based on the data listed in the above tables.

Table 28: Loading Pattern Radiotoxicity Data

LP #	TSEP	IRHRP
1	0.0048	-0.0140
2	0.0257	0.0725
3	0.0316	0.1568
4	0.0654	0.2800
5	0.0660	0.2841
6	0.0621	0.2966
7	0.0769	0.3855
8	0.0965	0.4659
9	0.0911	0.4670

5.3 RESULTS AND DISCUSSION FROM MULTIPLE BATCH ANALYSIS

The results of the multiple batch transmutation analysis are shown in Table 29. The results show that the neutronics behavior of the multiple batch core loading is much better than those for the loading patterns from single cycle burn discussed above. The k_{eff} range is much lower than the lowest for the loading patterns (0.043 vs .065 for LP7) and the peaking is also much lower than the lowest loading pattern (3.9 vs 5.5 for LP5). The results from the multiple batch analysis do not show the same trend observed in the single cycle analysis that the layouts with the better k_{eff} ranges also had the worst peaking factors and vice versa. However, the transmutation effectiveness of the multiple batch layout is much lower than those from the various loading patterns using single cycle burn discussed thus far. The multiple batch layout has the lowest TSEP and IRHRP compared to all the other loading patterns except LP1 which had negative values. The multiple batch layout was not very effective at reducing the radioactivity, radiotoxicity, or heat load of the TRUs and this showed up in the TSEP and IRHRP.

Table 29: Multiple Batch Analysis Results

Parameter	Value
Minimum K_{eff}	0.94905
Maximum K_{eff}	0.99221
Average K_{eff}	0.972395
K_{eff} Range	0.04316
Average Peaking Factor	3.0
Minimum Peaking Factor	2.3
Maximum Peaking Factor	3.9
Maximum Linear Heat Rate (W/cm)	554.3
Percent Reduction in Actinide Radioactivity	5.3
Percent of EOC Radioactivity from Fission Products	98.9
Percent Reduction in Actinide Heat Load	0.92
Percent of EOC Heat Load from Fission Products	98.79
Percent Reduction in Inhalation Radiotoxicity	6.10
Percent Reduction in Ingestion Radiotoxicity	3.59
TSEP	0.0264
IRHRP	0.0227

5.4 RESULTS AND DISCUSSION FROM MULTIPLE TARGETS ANALYSIS

As discussed in the introduction, the concept of implementing multiple targets in the ADS was proposed to mitigate power peaking in the core. In the present multiple target analyses, the assemblies loaded with all four TRUs, Np-Pu-Am-Cm (i.e., LP1 pattern) were utilized to simplify the calculations. The results of the multiple target core are given in Table 30. However, the multiple target core did not exhibit the kind of

neutronics qualities that the multiple batch core layout did. The k_{eff} range in the multiple target core was the worst observed, barely beating out LP5 with a k_{eff} range of 0.108. The peaking factor of the multiple target core averaged 5.2 throughout the various burnup steps analyzed. The idea behind the multiple target core was to reduce the peaking factors within the core by utilizing multiple source/target locations within the core. One possible reason the peaking factors did not improve as dramatically as expected for the multiple target core is the method used for calculating the peaking factors. When calculating the peaking factors, the assemblies with the target in them are avoided since the large central coolant channel changes the coolant's thermal capabilities for that assembly. Therefore, in the loading pattern analysis the center assembly was avoided because the target was located in the center assembly; however, in the multiple target layout, the center assembly is included but not three of the other assemblies. This could show an increase in the peaking factor since the center assembly will be the hottest assembly in the multiple target design. Also, in the multi target analysis the LP was not optimized and only one LP was analyzed compared to nine possibilities for the single target cores. Therefore, a direct comparison cannot be drawn and the data provided is merely for reference.

The transmutation effectiveness of the multiple target core layout are the worst observed in this study. The multiple target layout was ineffective at reducing the radioactivity or ingestion radiotoxicity of the TRUs present in the fuel. The heat load of the fuel was also increased during the cycle for the multiple target design.

Table 30: Multiple Target Analysis Results

Parameter	Value
Minimum K_{eff}	0.82292
Maximum K_{eff}	0.93086
Average K_{eff}	0.880864
K_{eff} Range	0.10794
Average Peaking Factor	5.2
Minimum Peaking Factor	4.3
Maximum Peaking Factor	6.1
Maximum Linear Heat Rate (W/cm)	867.0
Percent Reduction in Actinide Radioactivity	0.00
Percent of EOC Radioactivity from Fission Products	99.28
Percent Reduction in Actinide Heat Load	-5.9
Percent of EOC Heat Load from Fission Products	99.2
Percent Reduction in Inhalation Radiotoxicity	4.90
Percent Reduction in Ingestion Radiotoxicity	0.92
TSEP	-0.0003
IRHRP	-0.0252

6 CONCLUSIONS ON ELECTRON ADS

6.1 LOADING PATTERN ANALYSIS CONCLUSIONS

With the current legal limit set on Yucca Mountain, the currently operating fleet of power reactors in the United States will produce enough reactor waste to surpass Yucca Mountain's capacity by 2014.[2] Therefore, methods to enable more waste from power reactors to be stored safely in Yucca Mountain are being investigated. This thesis studies one of those possibilities, an electron accelerator based transmutation facility. The electron accelerator is directed at a neutron producing target within a subcritical core loaded with waste from LWR operations. In this thesis, the target was a cylinder of uranium 10cm thick with a diameter of 4cm. The subcritical core design utilized was a modification of the sodium cooled ALMR fast reactor loaded with TRU-Zr alloy fuel. In the study, ^{237}Np, ^{238}Pu, ^{239}Pu, ^{240}Pu, ^{241}Pu, ^{242}Pu, ^{241}Am, ^{242m}Am, ^{243}Am, ^{244}Cm, ^{245}Cm, ^{246}Cm, and ^{247}Cm were loaded into the ADS core for transmutation.

A large portion of this study was an investigation into the validity of various loading patterns possible by separating the elements present in the TRU mixture loaded into the core. Therefore, nine loading patterns were modeled in a twenty four month cycle at 500MWt. The results of the cycle were analyzed for neutronics and transmutation effectiveness characteristics.

Two values were investigated when looking at the neutronics behavior of the loading patterns analyzed. The k_{eff} range or swing during a cycle was the first value and the maximum peaking factor observed during a cycle was the second one. The results of the analysis showed that the loading patterns that maintained a constant k_{eff} more effectively also exhibited the highest peaking factors. As a reminder, note that the power

peaking calculations performed in this study ignored the power levels in assemblies containing a target. Assemblies with a target with have a larger cooling capacity due to the cooling channel for the target and therefore will have different thermodynamic properties than the rest of the heated channels. Even with ignoring the assemblies with targets in them, none of the loading patterns had sufficiently low peaking factors to be used for a final core loading pattern. However, the trends observed in the k_{eff} range and peaking factors should be noted. The k_{eff} range was minimized by placing the Np-Pu containing fuel assemblies on the periphery of the core. However, the core peaking factors were minimized by placing the Np-Pu assemblies in the interior of the core. Placement of Np-Pu assemblies in the innermost locations seemed to have high k_{eff} swings for any positioning of the Am and Cm assemblies. If Np-Pu assemblies are placed on the outside to minimize k_{eff} swings, then placing Am in the innermost assemblies further reduces the k_{eff} swing while placing Cm in the innermost assemblies helps to decrease the peaking factors observed. No loading pattern analyzed seemed to have a clear advantage over the rest due to its neutronics behavior.

The transmutation effectiveness of each loading pattern was determined by investigating multiple values and two parameters (i.e., TSEP, IRHRP) were used to combine the values into a single number representing the transmutation effectiveness. The ability of the ADS design to reduce the radioactivity, heat load, and radiotoxicity of the waste was investigated. The TSEP and IRHRP for each loading pattern were calculated to combine several of the above values together for a single representation to be used when comparing the loading patterns. Throughout the loading pattern transmutation effectiveness analysis, LP8 and LP9 stood out as the most effective loading

patterns for the current ADS design. LP7 was also consistently the third most effective loading pattern although it was always significantly less effective than LP8 and LP9. From these results, the placement of Cm in the innermost fuel assemblies appears to be the best approach for a loading pattern of this type. LP9 also exhibits a much lower k_{eff} swing than LP8, and a mid range peaking factor; therefore, LP9 was considered the most effective loading pattern analyzed. LP9 used Cm in the innermost fuel assemblies, Am in the second ring of fuel assemblies, and finally placed Np-Pu assemblies in the outermost locations.

6.2 OVERALL CONCLUSIONS ON ELECTRON ADS

The primary loading pattern analysis focused on cores using only one target and utilizing all fresh fuel every cycle for simplicity. However, a final ADS design may utilize multiple targets or multiple batches within a core design or layout. Therefore, two additional small studies were performed, one to investigate the use of multiple batches in the core and another to determine the effectiveness of using multiple targets in the core.

The multiple batch analysis produced results showing much better neutronics performance than the previous loading patterns analyzed. The k_{eff} swing and peaking factors in the multiple batch core were much lower than the lowest observed in the other loading patterns. This contradicts the trend seen in the other loading patterns in a single cycle study where a low k_{eff} swing was usually coupled with high peaking factors or vice versa. The downfall of the multiple batch core layout was its low transmutation effectiveness. The multiple batch core had lower transmutation effectiveness parameters than all of the previous loading patterns. This result may be due to the fact that the assemblies which had already experienced some burnup did not have as much mass of the

readily burnable TRUs due to previous burnup of those TRUs. However, given the much improved neutronics behavior of the multiple batch core, implementing some of its features in future core layouts should be seriously considered.

The loading pattern used in the multiple batch was not optimized to a great extent. The placement of the fresh fuel on the periphery of the core made it possible to achieve very low peaking levels; however, moving some of the fresh fuel further into the core can help achieve more efficient use of the neutrons in the core and possibly higher transmutation rates. The analysis for the multiple batch core also did not accurately represent the fission product production during each cycle; therefore any future analysis of a multiple batch ADS system should more accurately model individual fission products and attempt to further optimize the loading pattern when using multiple batches.

The multiple target based core design also exhibited very poor transmutation effectiveness. The multiple target core also did not exhibit better peaking factors as would be expected from the design. The main purpose of a multiple target system would be to help alleviate the peaking problem in ADS designs due to the large neutron source around the target. However, the multiple target design should not be abandoned without further study because there is most likely a more beneficial method of integrating the multiple target design and a loading pattern to create better neutronics behavior and transmutation effectiveness within the core. The multiple target analysis utilized assemblies loaded with all four TRUs, Np-Pu-Am-Cm, which as demonstrated in LP1's results is the least effective loading pattern. Therefore, when combining the multiple target core design with a more effective loading pattern such as one based on LP9, the results may follow expectations more closely.

7 COMPARISONS OF PROTON AND ELECTRON ADS

7.1 NEUTRON PRODUCTION EFFICIENCY

A major design consideration for an ADS is the type of particle accelerator to use. Proton accelerators have the major benefit of more efficient neutron production within the target. An electron accelerator based system can be expected to produce ~0.71neutrons/source particle.[10,12] A proton accelerator system with similar characteristics can achieve neutron production efficiencies in the range of 38 neutrons/source particle. The large difference in these factors comes into play when analyzing how much energy and ADS system can put towards the grid versus what must be supplied for the accelerator's operation. We can calculate the beam current required to support a subcritical system using the equation below from Reference 28.

$$I = \frac{\upsilon \cdot P \cdot 1.602 \cdot 10^{-19} C / p}{S \cdot \frac{k_{eff}}{1 - k_{eff}} \cdot Q_{ave}}$$

Where

I= the beam current (amps)

v= the number of neutrons produced/fission (~2.9 in a fast spectrum)

P= the power defined by user for each material

S= the number of neutrons leaking from the target per incident proton

K_{eff}= the effective multiplication factor obtained by the Monte Carlo neutron and photon transport code (MCNP)

$K_{eff}/(1-k_{eff})$= the ratio of the number of neutrons to the number of spallation neutrons because the number of fissions + the number of spallation neutrons must=1.0

Q_{ave}= the average recoverable energy released per fission (~200MeV)

The equation above assumes a proton accelerator system by using a value of ~30 for S. However, the equation can be used for an electron accelerator system by substituting the appropriate values. Using a value of S=0.718neutrons/source electron we can calculate the required accelerator beam current of various designs based on the k_{eff} of the system and thermal power. For example a system based on LP9 and utilizing the ADS target k_{eff}=0.97, the required accelerator beam current is 312mA. Currently most accelerators achieve beam currents much lower than 312mA. A maximum for accelerators is typically ~100mA. Therefore, either the energy of the accelerator must be increased to reduce the need for a high beam current or as shown below an improvement in the neutron production efficiency must be utilized. However, the current electron ADS design analyzed in this study utilizes a beam energy of 1GeV which is at the high end of the currently available accelerators in the world. Therefore, to meet the beam current and energy requirements of the current design, an accelerator more advanced than those currently in operation would be required. This is a serious disadvantage of the electron based system. Also, as shown below, even if the beam requirements were met, the low neutron conversion efficiency of the electron based system would result in a system that cannot send power to the grid without a k_{eff}=0.992 in the subcritical core design.

Utilizing the equation for beam current above, assuming a thermal to electrical conversion efficiency of 33%, and assuming an accelerator electricity to source particle energy conversion efficiency of 50%, an equation can be derived that determines the amount of thermal reactor power required to produce the electricity required to operate the accelerator. This new value, P_{recirc}, should be less than the thermal power of the system, P, in order to output power to the grid during operations. The equation to

calculate P_{recirc} is given below where $1*10^9$ represents the accelerator beam energy of 1GeV, 0.33 is the electrical production efficiency, and 0.5 represents the efficiency of the accelerator.

$$P_{recirc} = \frac{\upsilon * P * 1 * 10^9}{S * \left(\frac{k_{eff}}{1 - k_{eff}} \right) * 200 * 10^6 * 0.33 * 0.5}$$

In the current electron accelerator design, S=0.71neutrons/source particle. For this production efficiency the breakeven point (P_{recirc}=P) is when k_{eff}=0.992. However, most ADS designs typically strive for a starting k_{eff}=~0.97 to fully utilize the benefits of the accelerator including the safety characteristic associated with beam cutoff. A k_{eff}=0.992 is possible in the current design by utilizing a higher w/o of TRUs within the fuel design, but it would be more beneficial to obtain a higher neutron production efficiency to allow for the sale of electricity on the grid by the ADS system.

In order to obtain the goal of a k_{eff}=0.97 for the ADS system, the neutron production efficiency would have to be increased to S=2.718neutrons/source particle an increase of over 280%. The proton based ADS design utilizing an S=38neutrons/source particle has a breakeven point of k_{eff}=0.70. Therefore, from a neutron production efficiency point of view, the proton based ADS system is still superior to the electron based ADS. Another way to look at it is, if the systems were operated at k_{eff}=0.97, how much power could each system send to the grid as a net production of electricity. Manipulating the above equation for P_{recirc}, the LP9 conceptual design would need 165MW of electrical power from the grid to operate. On the other hand, a proton design utilizing an S=38 would put 238.6MW of electrical out to the grid. Therefore, while the

electron accelerator driven system needs power from the grid to operate, the proton ADS produces extra electricity that can be sold.

7.2 BURNUP CHARACTERISTICS

The electron ADS design developed exhibits a lower neutron conversion efficiency than a proton based system; however, the electron ADS may provide other benefits in transmutation not realized by the proton ADS. To investigate this possibility, the burnup characteristics of two electron ADS systems and two proton ADS systems were analyzed.

The first electron ADS system analyzed is based on the design developed in this thesis and utilizes loading pattern number nine (LP9) from above. The nomenclature 'LP9' will be used to reference this first electron ADS design. The LP9 system is a 500MWth system utilizing sodium cooling and a fast neutron spectrum. The total transmutation rate of this system is 372kg of TRUs per cycle. A cycle in the LP9 system is two years long.

The second electron ADS design was developed by Liu in Reference 12 and is denoted as the EADS design. The single target EADS system is utilized which operates at 4MWth. The EADS system also utilizes sodium cooling and a fast neutron spectrum. The total transmutation rate of this system is 1.8kg of TRUs per cycle. An EADS cycle length is 700days.

The first proton ADS system looked at is referenced within Reference 12 for comparison to the EADS and will be referenced as the PADS within the rest of this text. Within Reference 12, the PADS design was analyzed with two different fuel loadings;

however, for comparison purposes within this study, only fuel type I is considered. Fuel type I is based on JAERI's proposed alloy fuel type. The PADS system used a fast spectrum and sodium cooling as well. During a 700day cycle this system had a TRU burning rate of 45kg/cycle.

The second proton ADS system investigated differed from the other three designs compared below in that it utilizes a thermal neutron spectrum. The second proton ADS design is the Tier I design developed in Reference 23. This design utilizes molten salt as the fuel for its subcritical reactor, thus it is known as a molten salt reactor (MSR) and therefore MSR will be used to denote this second proton accelerator driven system. The MSR based system is 750MWth and has a TRU burnup rate of 300kg/yr.

The first step when analyzing the burnup characteristics of the four design listed above is to normalize the overall transmutation rates of the system to a common time length and energy generation. This information is listed in Table 31. To calculate these numbers, all of the designs assume sufficient neutron productions within their targets to maintain criticality within the system. Therefore, while the proton systems will be producing electricity for sale on the grid, the electron systems do not.

Table 31: Overall Transmutation Rates for Four ADS Systems

System:	LP9	EADS	PADS	MSR
Kgs of TRU burned/(yr*500MWth):	186	123.92	146.75	200

Table 31 shows the total TRU burnup of each system for an equivalent energy and time amount (500MWth system for 1yr). From these results, we can see that each of the four designs has relatively similar levels of total TRU burnup. The MSR and LP9

designs attain higher total burnup rates; however, these system designs are much larger and therefore can achieve higher burnup rates in the system. On the other hand, the EADS and PADS designs are smaller designs that demonstrate the benefits of lower overall capital costs and more attainable levels of accelerator beam currents. To put these overall transmutation rates into perspective, Table 32 gives the number of reactor-years for the 500MWth LP9 conceptual design would need to burn the amount of each element present in 63,000MTHM of spent nuclear fuel. Note that 63,000MTHM is the legal limit on Yucca Mountain for SNF from power reactors. Also, note that LP9 was loaded with Cm on the interior ring followed by Am and the Np-Pu assemblies on the outside of the core which would explain why Cm can be transmuted at a faster rate than Np-Pu.

Table 32: Reactor-years required to transmute 63,000MTHM of SNF worth of each element

Element:	Pu	Np	Cm	Am
Number of Reactor-years:	4097.091	3394.397	93.46705	1161.927

The second burnup characteristic that can be investigated for each design is the rate of burnup for each individual isotope. Data for each individual isotope can be found for the MSR in Reference 23. The data for LP9 was also collected. The rate of burnup for individual isotopes for LP9 and the MSR design is compiled below in Table 33.

Table 33: Individual Isotope Burnup Rates for MSR and LP9

TRU Isotope	MSR kg Burned per yr*500MWth Energy	LP9 kg Burned per yr*500MWth Energy
237Np	6.14	9.28
238Pu	26.13	10.76
239Pu	96.54	77.70
240Pu	43.68	35.47
241Pu	12.10	1.20

Table 33 Continued

242Pu	-1.09	5.58
241Am	9.5	20.56
242Am	-	2.81
243Am	-2.60	9.17
244Cm	-	13.03
245Cm	-	1.03
246Cm	-	-0.50
247Cm	-	-0.08

From Table 33, it is evident that the MSR design is more effective at burning the lower weight isotopes. However, this can be attributed to the use of a thermal spectrum within the MSR design. With the thermal spectrum, the fission to capture cross-section ratio is lower but the overall value of the fission and capture cross-sections can be higher. With the lower ratio, isotopes are more likely to experience a capture and increase in weight than in the fast spectrum system. Therefore, more lower weight isotopes are transmuted; however, a larger portion of them are transmuted to higher weight isotopes instead of experiencing fission. Therefore, as seen in the data the transmutation rate of the MSR for high weight isotopes is smaller than in LP9 because there is more production of the higher weight isotopes due to capture in the low weight isotopes.

The burnup rates of the four systems investigated demonstrates that larger systems generally achieve higher overall burnup rates per unit of thermal energy. The use of either an electron accelerator or proton accelerator does not seem to affect the transmutation abilities of the system. However, the smaller target size that can be utilized in an electron accelerator design allows for more flexibility in the design of the

subcritical core and target. Therefore, while the proton ADS has a much higher neutron production efficiency, the electron ADS has slightly more design flexibility and therefore, a possibly a higher or more targeted transmutation rate.

7.3 Economic and Timeline Considerations

Proton accelerator based designs have much higher neutron conversion efficiencies than the electron accelerator based systems. This results in a large economic benefit for the proton accelerator based systems since it allows more electrical energy to be sold on the grid by the proton accelerator based system. However, electron accelerator based systems have many other benefits that continue to promote the idea of an electron ADS as the possible system of choice. The capital cost of an electron accelerator is considered to be ~20% less than a comparable proton accelerator operating at the same energy level.[12] In Reference 12, the difference in capital cost for the electron accelerator and the proton accelerator is ~$50Million for accelerators of similar energies. While the accelerator is only one piece of the construction costs for an ADS design, keeping its cost down is necessary to allow the ADS designs to compete with other transmutation schemes. Therefore, the lower capital costs of the electron accelerator must be carefully considered in any economic analysis. Although the operational costs of the proton ADS will be significantly lower due to the ability to send electricity to the grid more efficiently, the lower capital cost of an electron based system may make it more attractive as a first of its kind deployment.

In the US, electron accelerators have a much larger operational experience base. This is the primary benefit of an electron ADS design since it translates into less accelerator trips and therefore less reactor shutdowns in the ADS. From the economic

perspective, a more stable operating scheme allows for a higher operating capacity, which is necessary for systems with high capital costs at the beginning of the project. Similarly to current power reactor operations within the US, higher operating capacities in any ADS will be a necessity for economic viability in today's diversified energy portfolio. From a safety perspective, unanticipated shutdowns are to be avoided whenever possible. Therefore, the reliability of the accelerator in an ADS is very important. Less unexpected shutdowns reduces the strain on the various components in a reactor system which increases safety and decreases O&M costs. Shutdowns cost money in terms of energy production and analysis costs and therefore the possibility of less accelerator trips during operations make the electron based system even more economically attractive.

The greater level of development associated with electron accelerators when compared to proton accelerators has another benefit besides operational stability and economics. The other benefit is the possibility of an earlier deployment of the ADS in the United States, especially for a possible test facility before full scale deployment. Many of the features of the design proposed above were chosen due to their more immediate availability for deployment in a US ADS system. For example, one of the reasons sodium was chosen as a coolant was due to the higher knowledge base associated with its use in fast reactors within the US. Lead based coolants, on the other hand may provide benefits above sodium, but they have not been used or testes extensively in the US and have significant short-term technological hurdles to overcome such as corrosion issues. The idea of enabling a quicker deployment for the electron ADS design developed in this study was utilized throughout the design process. Therefore, the

possibility of a feasible electron based ADS has been shown using technologies with at least some operating experience in the US.

8 CONCLUSIONS

As this study shows, even with very basic loading patterns the electron ADS transmutation facility can be effective at reducing the waste problem associated with LWR operation. Some design modifications such as burnable poisons or control elements would be needed to control the k_{eff} swings and peaking factors, but the general design is promising. An electron ADS has several benefits over the proton ADS in terms of economics and operational experience. However, the gap between neutron production efficiencies in the target is a major advantage for a proton accelerator based system because it allows more power to be sent to the grid to offset costs. The greater neutron conversion efficiency of the proton-based systems also avoid any problems due to higher beam current requirements than what is currently feasible in existing accelerators. The neutron production efficiency of the electron accelerator system should be further studied and more work should be done on loading patterns to alleviate the difference in neutron production in the targets of the two designs. The ability to deploy an electron ADS prototype facility more quickly and with lower capital costs could allow for the collection of experimental data to support further development of the electron ADS. However, without such further developmental support, in the long term the proton ADS designs show more promise due to the higher neutron production efficiency in the target. In this situation, small electron ADS facilities may still prove useful for targeted transmutation of specific isotopes. This is possible due to the smaller target size in the electron ADS. The smaller target size allows for a smaller overall system to be deployed efficiently which more be tailored for more specific applications while proton ADS system are utilized for the significant reductions in overall waste material from LWR power plants.

With these various future scenarios available, the further development of both proton is a must and development electron based ADS systems can provide benefits in faster deployment or small transmutation facilities.

REFERENCES

1. US DOE, Office of Civilian Radioactive Waste Management (February 2002). *Yucca Mountain Science and Engineering Report, Technical Information Supporting Site Recommendation Consideration, Revision 1*. http://www.ocrwm.doe.gov/documents/ser_b/index.htm

2. Kessler, J., EPRI (May 2006). *Program on Technology Innovation: Room at the Mountain; Analysis of the Maximum Disposal Capacity for Commercial Spent Nuclear Fuel in a Yucca Mountain Repository*.

3. Bennett, R. G., INEEL (February 2003). *Alternatives to Direct SNF Disposal: Advanced Nuclear Fuel Cycles.* 2003 NAE National Meeting Symposium in honor of Foreign Secretary Harold K. Forsen

4. National Research Council. *Nuclear Wastes: Technologies for Separations and Transmutation*. Washington, DC: National Academy Press, 1996.

5. ORNL DWG 95A-534. Oak Ridge National Laboratory, 1995.

6. ORNL DWG 92A-242. Oak Ridge National Laboratory, 1992.

7. US DOE (1999). *A Roadmap for Developing Accelerator Transmutation of Waste (ATW) Technology*, A Report to Congress. DOE/RW-0519.

8. IAEA (2004). *Implications of Partitioning and Transmutation in Radioactive Waste Management*. Tehcnical Report Series no. 435.

9. Bonnerot, J. M., et al (2005). Transmutation in reactor and aqueous corrosion resistance of technetium metal. *Journal of nuclear and radiochemical science, 6* (3), 287-290.

10. Yodersmith, S. (Summer 2006). *Electron Accelerator Driven System Target Design and Transuranic Loading Pattern Investigation.*

11. Brolly, A. and Vertes, P. *Transmutation: Towards Solving the Problem of Spent Nuclear Fuel*. Wigner Centennial Conference July 8-12, 2002. Paper no. 19.

12. Liu, Y. (May 2006). *A Study on the Feasibility of Electron-based Accelerator Driven Systems for Nuclear Waste Transmutation*

13. Frommberger, F. (February 2004). *Electron accelerator ELSA*. http://www-elsa.physik.uni-bonn.de/index_en.html

14. MIT Bates Linear Accelerator Center. (March 2007). http://mitbates.lns.mit.edu/bates/control/char

15. *Accelerator Sciences and Technologies Graduate & Undergraduate Research Opportunities at Jefferson Lab* http://www.jlab.org/div_dept/consortium/accel_brochure.pdf

16. MAMI Main Paramters (May 2007). http://www.kph.uni-mainz.de/B1/params.php

17. Leeman, C., Douglas, D., and Kraft, G. (2001) The Continuous Electron Beam Accelerator Facility: CEBAF at the Jefferson Laboratory. *Annual Review of Nuclear and Particle Science* (51) pp.413-50.

18. The Online Plotter for MCNP and ENDF Cross Section Data. http://atom.kaeri.re.kr/endfplot.shtml

19. Forsberg, C., *Molten-Salt Reactor Technology Gaps*. ICAPP '06 Paper #6295. June 4-8, 2006.

20. Crawford, D., Hayes, S., and Meyer, M. *Current US Plans for Development of Fuels for Accelerator Transmutation of Waste.* Argonne National Laboratory, USA.

21. Lee, B-O., Lee, B-S., and Park, W-S., *The Comparison of the Performance for the Alloy Fuel and the Inter-Metallic Dispersion Fuel by the MCSIS-H and the DIMAC*. Korea Atomic Energy Research Institute.

22. Spencer, B., *The Rush to Liquid Metal Coolants-Gimmick or Reasoned*. Proceedings of ICONE 8, April 2-6, 2000, Baltimore, MD USA. ASME 2000.

23. Bowman, C., *Accelerator-Driven Systems for Nuclear Waste Transmutation*. The Accelerator-Driven Neutron Applications Corporation.

24. MCNPX- Monte Carlo N-Particle Transport Code System for Multiparticle and High Energy Applications, Version 2.4.0. Los Alamos National Laboratory, September 2002.

25. Origen- Isotope Generation and Depletion Code, Version 2.2. Oak Ridge National Laboratory, July 1980.

26. MONTEBURNS- Automated, Multi-Step Monte Carlo Burnup Code System, Version 2.0. Los Alamos National Laboratory, July 2003.

27. Hill, R., and Khalil, H., *Physics Studies for Sodium Cooled ATW Blanket*. Argonne National Laboratory, USA.

28. H.R. Trellue, E.J. Pitcher, P. Chodak Iii, D. Bennett Los Alamos National Laboratory, Los Alamos, New Mexico, United States of America. *Two-Tiered Approach For Lightwaterreactor Waste Disposition Using Existing Lightwater Reactors And A Minor Actinide Burner.*